



MASTER THESIS

---

# Optimization of Neural Network

---

*Author:*  
Martin BULÍN MSc.

*Supervisor:*  
Ing. Luboš ŠMÍDL Ph.D.

*A thesis submitted in fulfillment of the requirements  
for the degree of Engineer (Ing.)*

*in the*

Department of Cybernetics

May 7, 2017

## Declaration of Authorship

I, Martin BULÍN MSc., declare that this thesis titled, “Optimization of Neural Network” and the work presented in it are my own. The main methods follow on my work presented in (Bulín, 2016), however the workload of this thesis is different.

I confirm that:

- Where any part of this thesis has previously been submitted for a degree or any other qualification at this University or any other institution, this has been clearly stated.
- Where I have consulted the published work of others, this is always clearly attributed.
- Where I have quoted from the work of others, the source is always given. With the exception of such quotations, this thesis is entirely my own work.
- I have acknowledged all main sources of help.

Signed:

---

Date:

---

*“Look deep into nature, and then you will understand everything better.”*

A. Einstein

UNIVERSITY OF WEST BOHEMIA

# *Abstract*

Faculty of Applied Sciences

Department of Cybernetics

Engineer (Ing.)

## **Optimization of Neural Network**

by Martin BULÍN MSc.

abstract text...

# *Acknowledgements*

acknowledgements text...

# Contents

<b>Abstract</b>	<b>iii</b>
<b>1 Introduction</b>	<b>1</b>
1.1 State of the Art . . . . .	1
1.2 Thesis Objectives . . . . .	1
1.3 Thesis Outline . . . . .	1
<b>2 Methods</b>	<b>2</b>
2.1 Classification Method . . . . .	2
2.2 Network Pruning . . . . .	8
2.3 Feature Selection . . . . .	10
2.4 Speech Data Gathering . . . . .	11
<b>3 Examples</b>	<b>16</b>
3.1 XOR Function . . . . .	16
3.2 Unbalanced Feature Information . . . . .	19
3.3 Rule-plus-Exception . . . . .	22
3.4 Michalski's Trains . . . . .	24
3.5 Handwritten Digits (MNIST) . . . . .	26
3.6 Phonemes (Speech Data) . . . . .	31
<b>4 Discussion</b>	<b>37</b>
4.1 Methods Recapitulation . . . . .	37
4.2 Comparison of Pruning Methods . . . . .	37
4.3 Future Work . . . . .	38
<b>5 Conclusion</b>	<b>39</b>
<b>Bibliography</b>	<b>40</b>
<b>A1 Supplementary Data</b>	<b>41</b>
<b>A2 Structure of the Workspace</b>	<b>45</b>
<b>A3 Implementation</b>	<b>46</b>
<b>A4 Code Documentation</b>	<b>47</b>

# List of Figures

2.1	A general dense feedforward neural network. . . . .	2
2.2	A model neuron . . . . .	3
2.3	Transfer functions: <i>Sigmoid</i> and <i>Tanh</i> . . . . .	4
2.4	Training process flowchart. $T_1$ : Threshold for a terminating condition based on the prediction error (Eq. (2.19)). If the error is reduced to be lower $T_1$ , the learning process is stopped and the model is considered trained. $T_2$ : Threshold for a terminating condition based on the number of epochs. The learning process is stopped after $T_2$ epochs, no matter how successful the training has been. . . . .	5
2.5	Pruning Algorithm: problem formulation. . . . .	8
2.6	The flowchart of pruning one synapse, demonstration of parameter retrain. . . . .	8
2.7	Network pruning proceeder. . . . .	9
2.8	Framing a sound signal. . . . .	12
2.9	Mel Filterbank of 40 filters in Hertz-axis. . . . .	13
2.10	Forming a sample, illustration of parameter <code>border_size</code> ( <code>bs</code> ). . . . .	14
2.11	Forming a sample, illustration of parameter <code>context_size</code> ( <code>cs</code> ). . . . .	14
2.12	Example of building a feature vector with <code>context_size</code> $cs = 2$ . . . . .	15
2.13	Using three disjunctive sets of data for a general machine learning process. . . . .	15
3.1	Optimal network architectures producing the XOR function. . . . .	17
3.2	The XOR dataset. . . . .	17
3.3	Illustration of the pruning procedure applied on XOR dataset (selected observation). . . . .	18
3.4	Pruning results for XOR dataset. . . . .	18
3.5	The UFI dataset. . . . .	19
3.6	Expected pruning of input-hidden synapses (UFI problem). . . . .	19
3.7	Results of pruning (see Fig. 3.6) input-hidden synapses (100 observations, UFI example). . . . .	20
3.8	Weight change in training for the remaining input-hidden synapses (100 observations). . . . .	21
3.9	Expected pruning of input-hidden synapses (RPE problem). . . . .	22
3.10	Results of pruning (see Fig. 3.9) input-hidden synapses (100 observations, RPE example). . . . .	23
3.11	Weight change in training for input-hidden synapses (100 observations, RPE example). . . . .	23
3.12	Michalski's train problem. . . . .	24

3.13	Results of feature selection by the pruning algorithm (train example). The labels corresponds with feature indices in Table 3.5. . . . .	25
3.14	Examples of MNIST dataset. . . . .	26
3.15	Confusion matrix (MNIST, testing data). . . . .	27
3.16	Illustration of the pruning procedure applied on MNIST dataset (selected observation). Required accuracy: 97%. . .	27
3.17	Evaluation (accuracy and error computation) time for all data groups (pruned vs. full net). . . . .	28
3.18	Minimal number of features and synapses to get required classification accuracy (MNIST data). . . . .	28
3.19	Result of network pruning and path tracking, MNIST data, accuracy: 50%. . . . .	29
3.20	Result of network pruning and path tracking (shown 17 <sup>th</sup> hidden neuron only), MNIST data, accuracy: 97%. . . . .	29
3.21	Used features for individual classes, MNIST data, accuracy: 97%. . . . .	30
3.22	Test MSE' (Eq. (2.19)) for various parameters $bs$ and $cs$ ( $ns = 1000$ , 5 observations, see Table A1.1). . . . .	31
3.23	Randomly selected sample for each phoneme, $cs = 0$ . . . . .	32
3.24	Average sample for each phoneme, $cs = 0$ . . . . .	32
3.25	Randomly selected sample for each phoneme, $cs = 3$ . . . . .	33
3.26	Representation of individual phonemes in the 2D bottleneck layer (selected phonemes). . . . .	34
3.27	Confusion matrix of the classification results on the speech dataset. . . . .	35
3.28	Illustration of the pruning procedure applied on SPEECH dataset (selected observation). Required accuracy: 50%. . .	35
4.1	MNIST, req_acc = 0.95, retraining: 5 epochs . . . . .	37
4.2	MNIST, req_acc = 0.95, no retraining . . . . .	38
A1.1	Average sample for each phoneme, $cs = 3$ . . . . .	44
A1.2	Trained bottleneck network (speech dataset): confusion matrix. . . . .	44



# List of Tables

2.1	Czech phonetic alphabet. . . . .	11
2.2	Example of labeled recording. . . . .	13
3.1	XOR function. . . . .	16
3.2	Experiment settings for the XOR example. . . . .	18
3.3	Experiment settings for the UFI example. . . . .	20
3.4	Experiment settings for the RPE example. . . . .	22
3.5	Features describing a train. . . . .	24
3.6	Feature vectors for different train types. . . . .	24
3.7	Experiment settings for the train example. . . . .	25
3.8	Settings for training a dense feedforward net on the MNIST dataset. . . . .	26
3.9	Training results on MNIST dataset. . . . .	26
3.10	Experiment settings for the MNIST example. . . . .	27
3.11	Speech dataset: experiment settings for determination of op- timal $bs$ and $cs$ . . . . .	31
3.12	Phonemes: dataset and learning parameters. . . . .	33
A1.1	Datasets generated for the <i>Phonemes</i> example (section 3.6). .	42
A1.2	Complete results of finding speech dataset parameters $bs$ and $cs$ . MSE' (Eq. (2.19)) after training. . . . .	43

# List of Abbreviations

<b>AI</b>	<b>A</b> rtificial <b>I</b> ntelligence
<b>ANN</b>	<b>A</b> rtificial <b>N</b> eural <b>N</b> etwork
<b>DCT</b>	<b>D</b> iscrete <b>C</b> osine <b>T</b> ransform
<b>DFT</b>	<b>D</b> iscrete <b>F</b> ourier <b>T</b> ransform
<b>GDA</b>	<b>G</b> radient <b>D</b> escent <b>A</b> lgorithm
<b>HMMs</b>	<b>H</b> idden <b>M</b> arkov <b>M</b> odels
<b>MNIST</b>	<b>M</b> odified <b>N</b> ational <b>I</b> nstitute of <b>S</b> tandards and <b>T</b> echnology
<b>MFCCs</b>	<b>M</b> el <b>F</b> requency <b>C</b> epstral <b>C</b> oefficients
<b>MSE</b>	<b>M</b> ean <b>S</b> quared <b>E</b> rror
<b>NN</b>	<b>N</b> eural <b>N</b> etwork
<b>PA</b>	<b>P</b> runing <b>A</b> lgorithm
<b>RPE</b>	<b>R</b> ule <b>P</b> lus <b>E</b> xception
<b>UFI</b>	<b>U</b> nbalanced <b>F</b> eature <b>I</b> nformation
<b>XOR</b>	<b>eX</b> clusive <b>OR</b>
<b>WSF</b>	<b>W</b> eight <b>S</b> ignificance <b>F</b> actor

# Chapter 1

## Introduction

Introduction text...

### 1.1 State of the Art

State of the art text... (Reed, 1993)

Karnin method principle

OBD method principle

### 1.2 Thesis Objectives

Thesis objectives text...

### 1.3 Thesis Outline

Thesis outline text...

## Chapter 2

# Methods

The methods of this work are introduced here. Section 2.1 describes the classification model and the learning method. In section 2.2 the developed network pruning algorithm is introduced and also the dimensionality reduction in pruned networks is shown. Section 2.3 comes with the feature selection method using a procedure called *pathing* and additionally, some ideas of how to use remaining weights in minimal structures are suggested. Finally, section 2.4 is devoted to the process of speech data gathering.

Section 2.1 moreover specifies a generally known approach. Sections 2.2 - 2.3 are partially based on (Bulín, 2016), but the methods are further elaborated. Section 2.4 is highly supported by (Šmídl, 2017).

### 2.1 Classification Method

The classification in this study is performed by dense feedforward neural networks. An illustration of a general network structure is in Fig. 2.1. Note that the structure is fully connected, meaning that each neuron is connected to all neurons in the next layer.

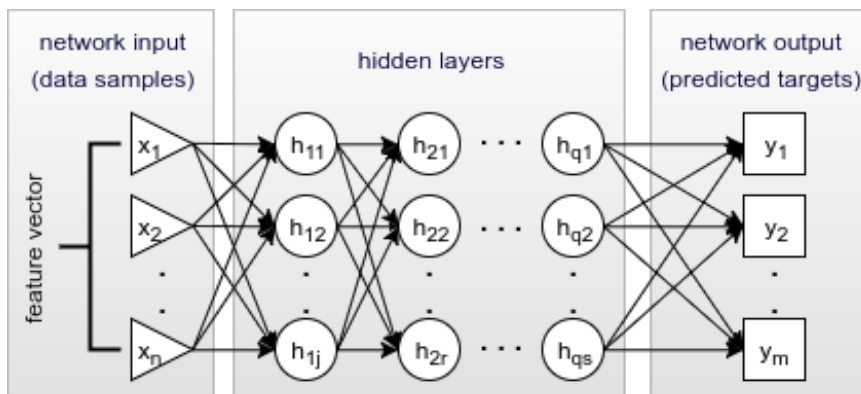


FIGURE 2.1: A general dense feedforward neural network.

The number of input units  $n$  is determined by the problem dimension. The number of classes gives the number of output units  $m$  (see the established conventions in appendix A3). In this study, we mostly use a simple hidden structure, usually with one hidden layer ( $q = 1$ ).

## Neuron Principle

The behaviour of artificial neurons follows our understanding of how biological neurons work. One unit has multiple inputs and a single output (Rosenblatt, 1958). A model of neuron is shown in Fig. 2.2. The diagram complies with the following notation:

$neuron_k^{(i)}$  :  $k^{th}$  neuron in  $i^{th}$  layer

$a_k^{(i)}$  : activity of  $k^{th}$  neuron in  $i^{th}$  layer

$w_{k,l}^{(i)}$  : weight of synapse connecting  $l^{th}$  neuron in  $(i-1)^{th}$  layer with  $k^{th}$  neuron in  $i^{th}$  layer

$b_k^{(i)}$  : bias connected to  $k^{th}$  neuron in  $i^{th}$  layer

$z_k^{(i)}$  : activation of  $k^{th}$  neuron in  $i^{th}$  layer

$f(\cdot)$  : transfer function (Eq. (2.3); Fig. 2.3)

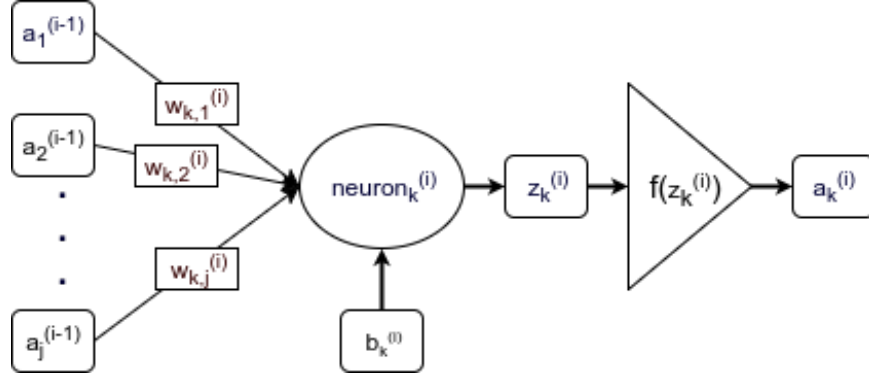


FIGURE 2.2: A model neuron

Assuming  $j$  being the number of neurons in  $(i-1)^{th}$  layer, the activation of  $neuron_k^{(i)}$  is computed as in Eq. (2.1)

$$z_k^{(i)} = \sum_{l=1}^j [a_l^{(i-1)} \cdot w_{k,l}^{(i)}] + b_k^{(i)} \quad (2.1)$$

Then we get the neuron activity by mapping its activation into a finite interval using a transfer function  $f(\cdot)$  - see Eq. (2.2).

$$a_k^{(i)} = f(z_k^{(i)}) \quad (2.2)$$

The *Sigmoid* function (Eq. (2.3)) keeps neuron activities in the  $[0, 1]$  interval and is used by default in this work. Alternatively, one could use the hyperbolic tangent ( $\tanh(\cdot)$ ) function, which maps the input into the  $[-1, 1]$  interval.

$$f(z) = \frac{1}{1 + e^{-z}} \quad (2.3)$$

The two basic transfer functions are shown in Fig. 2.3.

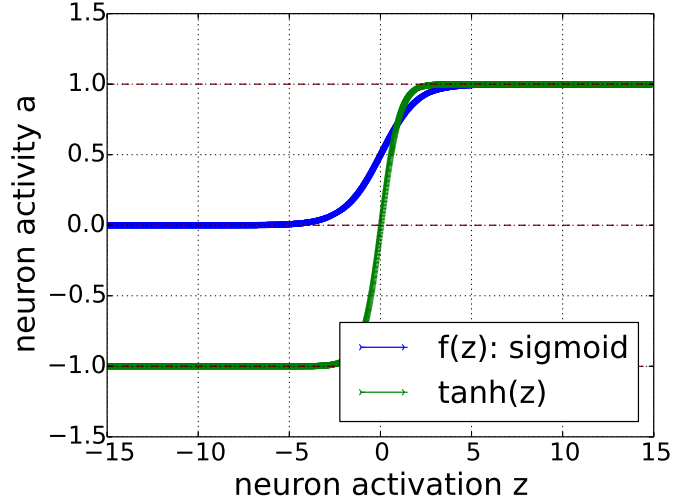


FIGURE 2.3: Transfer functions: *Sigmoid* and *Tanh*

## Notation

The work of a neural network is all done by matrix calculations. Therefore we need to introduce a notation used in this study. Detailed examples of the itemized matrices can be found in appendix A3.

- $n$  : number of input neurons (problem dimension; size of one sample);
- $m$  : number of output neurons (classes);
- $p$  : number of samples;
- $q$  : number of hidden layers;
- $X$  : network input:  $n$ -by- $p$  matrix;
- $W^{(i)}$  :  $r$ -by- $s$  matrix of weights for synapses connecting  $s$  neurons in  $(i-1)^{th}$  layer to  $r$  neurons in  $i^{th}$  layer;
- $B^{(i)}$  : vector of  $r$  biases for  $r$  neurons in  $i^{th}$  layer;
- $Z^{(i)}$  :  $r$ -by- $p$  matrix of activations for  $r$  neurons in  $i^{th}$  layer for all samples;
- $A^{(i)}$  :  $r$ -by- $p$  matrix of activities of  $r$  neurons in  $i^{th}$  layer for all samples;
- $\Delta^{(i)}$  :  $r$ -by- $p$  matrix of errors on neurons in  $i^{th}$  layer for all samples;
- $Y$  : predicted network output for all samples:  $m$ -by- $p$  matrix ( $Y = A^{(q)}$ )
- $U$  : desired network output (targets) for all samples:  $m$ -by- $p$  matrix

## Learning Algorithm

Feedforward networks are trained by the common *Backpropagation* method illustrated by the flowchart in Fig. 2.4.

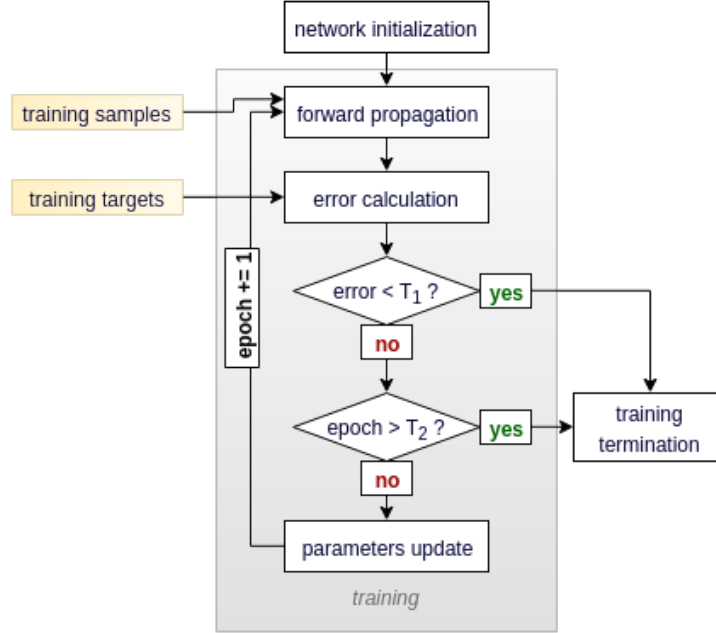


FIGURE 2.4: Training process flowchart.  $T_1$ : Threshold for a terminating condition based on the prediction error (Eq. (2.19)). If the error is reduced to be lower  $T_1$ , the learning process is stopped and the model is considered trained.  $T_2$ : Threshold for a terminating condition based on the number of epochs. The learning process is stopped after  $T_2$  epochs, no matter how successful the training has been.

In case of feedforward neural networks, the goal is to find optimal values for two groups of parameters - *weights* ( $W$ ) and *biases* ( $B$ ). The key idea lies in the optimization method called *Gradient Descent Algorithm* (*GDA*).

At first, a batch of samples  $X$  is (forward) propagated through a network to get the network's prediction  $Y$ .

$$Z^{(1)} = W^{(1)} \cdot X + B^{(1)} \quad (2.4)$$

$$A^{(1)} = f(Z^{(1)}) \quad (2.5)$$

$$A^{(i)} = f(W^{(i)} \cdot A^{(i-1)} + B^{(i)}) \quad (2.6)$$

$$Y = A^{(q)} = f(W^{(q)} \cdot A^{(q-1)} + B^{(q)}) \quad (2.7)$$

Then, having the known targets (supervised learning), we compute a prediction error on every output neuron for every sample and store those errors in the  $m$ -by- $p$  matrix  $E$ .

$$E = \frac{1}{2} \|U - Y\|^2 \quad (2.8)$$

Now it is time to use *GDA* to find such settings of  $W$  and  $B$  that makes  $E$  minimal. The details of the *Backpropagation* procedure are well described in (Nielsen, 2017). The envelope of the algorithm includes these steps:

1. *find the derivative of the transfer function (assuming Sigmoid);*

$$f'(z) = f(z) \cdot (1 - f(z)) \quad (2.9)$$

2. *backpropagate the prediction error throught the network;*

$$\Delta^{(q+1)} = (U - Y) \times f'[Z^{(q+1)}] \quad (2.10)$$

$$\Delta^{(i)} = \left[ \left[ W^{(i+1)} \right]^T \cdot \Delta^{(i+1)} \right] \times f'[Z^{(i)}] \quad (2.11)$$

3. *find the optimal parameter changes;*

Every sample  $\xi$  has a vote  $dW_{(\xi)}^{(i)}$  (resp.  $dB_{(\xi)}^{(i)}$ ) on how the parameters  $W^{(i)}$  (resp.  $B^{(i)}$ ) should change to get the minimal error and the result is then obtained as a compromise of those votes.

Index  $(i)$  indicates the layer. Consider  $\Delta_{(\xi)}^{(i)}$  be the  $\xi^{th}$  column of the  $\Delta^{(i)}$  matrix, which corresponds to the  $\xi^{th}$  sample. Analogically,  $A_{(\xi)}^{(i-1)}$  is the  $\xi^{th}$  column of the activation matrix  $A^{(i-1)}$  in the  $(i-1)^{th}$  layer. Then we get the votes as:

$$dW_{(\xi)}^{(i)} = A_{(\xi)}^{(i-1)} \cdot \left[ \Delta_{(\xi)}^{(i)} \right]^T \quad (2.12)$$

$$dB_{(\xi)}^{(i)} = \Delta_{(\xi)}^{(i)} \quad (2.13)$$

4. *update the parameters.*

At this point we introduce the first parameter of the learning process called `batch_size`. It states how many votes are processed together to make one update of the parameters. If `batch_size` = 1, we are talking about a *sequential learning*. In this case, each vote is applied to update the parameters before any other votes are computed (Eq. (2.14);  $t$  refers to a moment in time).

$$dW^{(i)}(t) = dW_{(\xi)}^{(i)} \quad (2.14)$$

In this work, we usually use *batch learning* (`batch_size` > 1).

$$dW^{(i)}(t) = \sum_{\xi}^{batch\_size} dW_{(\xi)}^{(i)} \quad (2.15)$$

Equations 2.14 and 2.15 works analogically for the biases.



The second parameter of the learning procedure is called `learning_rate` ( $\mu$ ) and is usually set  $0 < \mu \ll 1$  in order to deal with GDA problems (see (Nielsen, 2017)). The update of the parameters is then done as follows:

$$W^{(i)}(t+1) = W^{(i)}(t) + \mu \cdot dW^{(i)}(t) \quad (2.16)$$

$$B^{(i)}(t+1) = B^{(i)}(t) + \mu \cdot dB^{(i)}(t) \quad (2.17)$$

When the votes of all samples are applied, the learning epoch ends (see Fig. 2.4). The maximal number of epochs and the maximal required error (see Fig. 2.4) are also parameters of the learning procedure. To list them all:

- `batch_size`
- `learning_rate` ( $\mu$ )
- `n_epoch`
- `max_error` ( $MSE'$ ; Eq. (2.19))

## Network Evaluation

We use two measures to evaluate the network training: error and accuracy. The error measure is based on the standard *Mean Squared Error* ( $MSE$ ) given by Eq. (2.18).

$$MSE = \frac{1}{2p} \sum_{\xi=1}^p \|y_{\xi} - u_{\xi}\|^2 \quad (2.18)$$

where  $y_{\xi}$  is the prediction for sample  $\xi$  and  $u_{\xi}$  its corresponding (known) target. Both are vectors of length  $m$  (number of classes).

In this study we rather use the measure given by Eq. (2.19), because it makes a fair comparison of problems with different number of classes.

$$MSE' = \frac{1}{2pm} \sum_{\xi=1}^p \sum_{\theta=1}^m (y_{\xi,\theta} - u_{\xi,\theta})^2 \quad (2.19)$$

The classification accuracy is computed with Eq. (2.20).

$$acc = \frac{1}{p} \sum_{\xi=1}^p \psi, \quad \psi = \begin{cases} 1, & \text{argmax}(y_{\xi}) = \text{argmax}(u_{\xi}) \\ 0, & \text{otherwise} \end{cases} \quad (2.20)$$

The classification result is often shown by a confusion matrix (well explained in (Buitinck et al., 2013)). The testing is usually done on different data samples than used for training - see Fig. 2.13.

## 2.2 Network Pruning

The rule of thumb in classification with feedforward neural networks is using a fully connected structure - every unit is connected to all units in the next layer.

Pruning methods work with the hypothesis that some of the synapses in fully connected networks do not contribute to the classification and so their removal would not cause a significant accuracy drop. The problem (graphically illustrated in Fig. 2.5) is to distinguish those redundant synapses from the important ones.

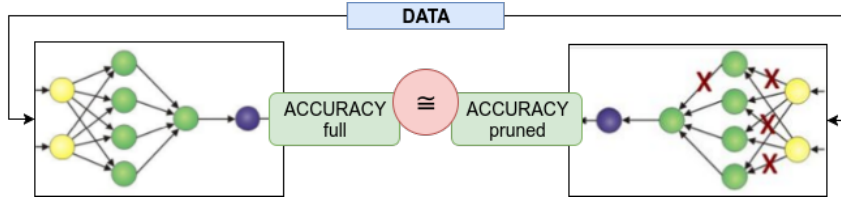


FIGURE 2.5: Pruning Algorithm: problem formulation.

There are several ways of how to estimate the importance of synapses (see section 1.1). In this study we introduce a measure called *weight significance factor* (WSF) given by Eq. (2.21).

$$WSF(w_{k,l}^{(i)}) = |w_{k,l}^{(i)}(t_f) - w_{k,l}^{(i)}(0)| \quad (2.21)$$

where  $w_{k,l}^{(i)}(t_f)$  is the weight of synapse coming to  $k^{th}$  neuron in the  $i^{th}$  layer from  $l^{th}$  neuron in  $(i-1)^{th}$  layer after training ( $t_f$ : time final). Analogically,  $w_{k,l}^{(i)}(0)$  is the initial weight of the same synapse before training. We compare these two values and get the change in weight over the training process. The key idea is that the redundant synapses do not change their weights over the training. Therefore, those synapses with low WSF are considered less important than those with high WSF.

### Realization of the Pruning Proceeder

The general recipe of how to prune a synapse is illustrated in Fig. 2.6.

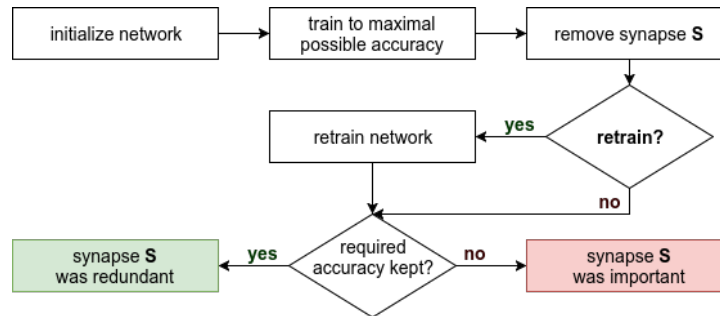


FIGURE 2.6: The flowchart of pruning one synapse, demonstration of parameter retrain.

Fig. 2.6 introduced the first parameter of the pruning process called `retrain`. We make it *True* if we want to retrain the pruned network (without the cut synapse) before checking the accuracy drop. In practice, we are able to set the exact number of epochs we want the net to retrain.

The required accuracy (`req_acc`) is the second parameter. In some cases we want to give up some of the accuracy in exchange for well pruned network in order to see some patterns in it. This parameter sets the minimal accuracy the network must have so that we can treat the lastly cut synapses as unimportant. The accuracy is checked on development data, while the training is performed on training data (see Fig. 2.13).

So far we gave a recipe of how to prune one synapse. Of course, we cannot check all the synapses one by one using the approach in Fig. 2.6. Instead we cut out multiple synapses at once before checking the accuracy drop. In fact, network pruning is an iterative procedure with some guessing. The first guess is the order in which we prune the synapses and the second guess is how many should we prune at once.

The order of the synapses is determined by the WSF (Eq. (2.21)) - the key idea of our pruning algorithm. Each time before pruning, all the synapses are sorted by their WSF values.

To estimate the number of synapses to cut at once we use percentiles - see Fig. 2.7.

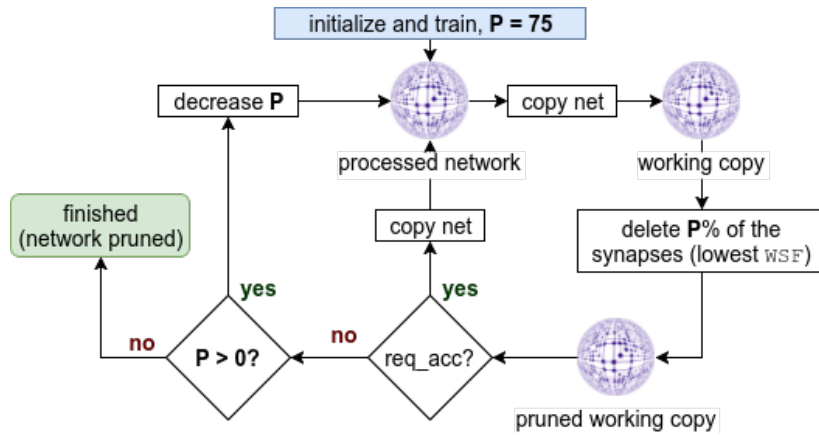


FIGURE 2.7: Network pruning procedure.

The percentile level is set to  $P = 75$  at the beginning. Hence the algorithm tries to prune 75% of the synapses (those with low WSF) in the first pruning step. Then the accuracy drop is checked (with or without retraining). If the accuracy dropped, we decrease the percentile level  $P$  and try to delete less synapses in the next step.

At this point we introduce another parameter of the pruning procedure called `percentile_levels`, which is an array specifying the levels we try (e.g. `percentile_levels = (75, 50, 30, 20, 0)`). The last level in this array is always zero. When  $P = 0$  we delete only the one synapse; the one with the lowest WSF. In this manner, at some point of the pruning process, the algorithm will come to removing only one synapse at once and if only a single synapse has been removed during the last pruning step and the accuracy has been

broken, it means that even this single synapse with the least change in weight is important for classification. Therefore, the pruning is stopped and the current net structure (including this last synapse) is saved as the minimal structure. Therefore, the algorithm is finite and it also guarantees that the classification accuracy does not drop.

To sum up the parameters of the pruning procedure:

- `retrain`
- `req_acc`
- `percentile_levels`

## Dimensionality Reduction

### 2.3 Feature Selection

Minimal network structure text...

Pathing in Net (Feature Selection)

Feature Energy computation

## 2.4 Speech Data Gathering

The presented methods are tested on several examples (chapter 3) and one of them rests in classification of phonemes. By definition a phoneme is one of the units of sound that distinguish one word from another in a particular language (Wikipedia, 2004). We focus on Czech language and consider 40 phonemes listed in Table 2.1. This section describes the way of gathering such phonemes and building a dataset for classification.

<i>sound</i>	<i>phoneme</i>	<i>example</i>	<i>sound</i>	<i>phoneme</i>	<i>example</i>	<i>sound</i>	<i>phoneme</i>	<i>example</i>
a	a	máma	ch	x	chyba	ř	R	moře
á	A	táta	i	i	pivo	ř	Q	tři
au	Y	auto	í	I	víno	s	s	osel
b	b	bod	j	j	voják	š	S	pošta
c	c	ocel	k	k	oko	t	t	otec
č	C	oči	l	l	loď	ť	T	kutil
d	d	dům	m	m	mír	u	u	rum
ď	D	děti	n	n	nos	ú (ů)	U	růže
e	e	pes	n	N	banka	v	v	vlak
é	E	lépe	ň	J	laň	z	z	koza
eu	F	eunuch	o	o	bok	ž	Z	žena
f	f	facka	ou	y	pouto		_sil_	(silence)
g	g	guma	p	p	prak			
h	h	had	r	r	rak			

TABLE 2.1: Czech phonetic alphabet.

The generation of a speech dataset consists of the following steps, where the work done in steps 1 – 3 is taken over from (Šmídl, 2017).

1. acquisition of real voice recordings;
2. feature extraction from the sound signals (parameterization);
3. labeling the data;
4. definition of one sample;
5. splitting samples into training/development/testing sets.

### Acquisition of Voice Recordings

The phoneme dataset is made of real speech recordings from a car interior environment, provided by (Škoda, ?? ref). We are talking about simple voice instructions for a mobile phone or a navigation system, many of them are names of people, streets or towns only. In total 14523 recordings (.wav files) of various length (and so number of phonemes) were obtained.

### Parameterization

The goal of parameterization is to represent each recording by a vector of features. A commonly known procedure based on MFCCs is used. A nice detailed explanation of this method can be found e.g. in (Lyons, 2009).

The idea behind MFCCs originates in the fact that a shape of human vocal tract (including tongue, teeth etc.) determines what sound comes out. The shape of the vocal tract manifests itself in the envelope of the short time power spectrum, and the job of MFCCs is to accurately represent this envelope.

The parameterization workflow is summarized by these steps:

1. *splitting the signal into short frames;*

Fig. 2.8 illustrates how a sound signal is splitted into short frames. The parameters are

$$\begin{aligned} \text{frame\_size} &= 0.025 \text{ s} = 25 \text{ ms} \\ \text{frame\_shift} &= 0.01 \text{ s} = 10 \text{ ms} \end{aligned}$$

Using the sampling frequency  $f_s = 8 \text{ kHz}$ , we get frames of length 200.

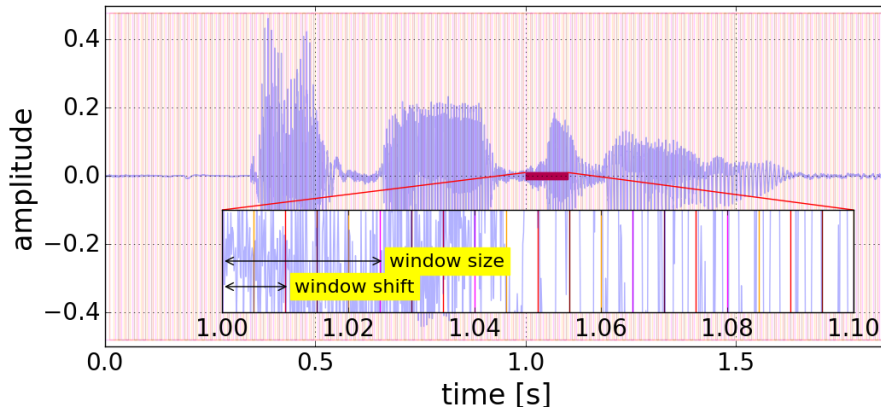


FIGURE 2.8: Framing a sound signal.

We assume each frame captures one possible shape of the human vocal tract and therefore is capable of carrying one phoneme only. The next steps are applied for every single frame.

2. *calculation of the periodogram estimate of the power spectrum;*

The aim is to identify which frequencies are present. In order to do so, we apply the Hamming window and perform the discrete Fourier Transform (DFT; Eq. (2.22)).

$$S(k) = \sum_{n=0}^{N-1} s_n \cdot e^{-2\pi i \frac{kn}{N}}, \quad k = 0, \dots, N-1 \quad (2.22)$$

, where  $N$  (in this case  $N = 200$ ) is the signal length. Then we take the absolute value  $|S(k)|$ .

3. *application of the mel filterbank to the power spectra, summation of the energy in each filter, taking a logarithm of the result;*

Next, we use a filterbank of triangle filters (illustrated in Fig. 2.9) predefined on the transmitted band ( $bw = \frac{f_s}{2} = 4 \text{ kHz}$ ) to get a single

value per filter. We use 40 filters, therefore, each frame is now described by a vector of 40 numbers.

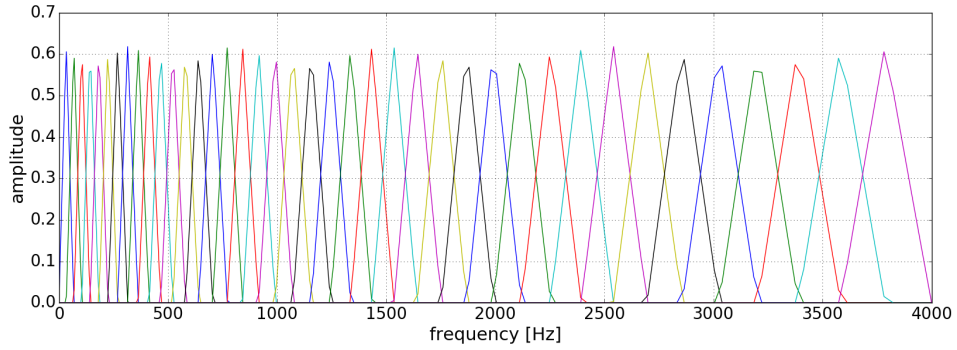


FIGURE 2.9: Mel Filterbank of 40 filters in Hertz-axis.

Finally, a logarithm of the result is taken and considered as a description of the frame (phoneme). Usually, a discrete Cosine Transform (DCT) is applied at the end, however, it is not done in this work. The result of a signal parameterization is a matrix shown in Eq. (2.23).

$$recording\_params = \begin{bmatrix} f_{11} & f_{12} & f_{13} & \dots & f_{1F} \\ f_{21} & f_{22} & f_{23} & \dots & f_{2F} \\ \vdots & \vdots & \vdots & \ddots & \vdots \\ f_{W1} & f_{W2} & f_{W3} & \dots & f_{WF} \end{bmatrix} \quad (2.23)$$

, where  $F = 40$  is the number of filters and  $W$  is the number of frames (windows) depending on the duration of a recording. Value  $f_{12}$  then belongs to the feature computed with the second filter in the first frame.

## Data Labeling

We perform a supervised learning method, hence the data must be labeled. To the so a speech recognition method based on Hidden Markov Models (HMMs) from (Šmídl, 2017) is used. It labels the frames of each recording as shown on an example in Table 2.2.

recording_name		
<i>frame_in</i>	<i>frame_out</i>	<i>phoneme</i>
0	16	_sil_
16	25	a
25	32	n
32	44	o
44	65	_sil_

TABLE 2.2: Example of labeled recording.

It says that features extracted from this recording consist of 9 fourty-dimensional vectors representing phoneme "a", 7 vectors of phoneme "n", etc.

### Forming a Sample

The 40 phonemes listed in Table 2.1 are naturally labels of classes, so we have a fourty-class classification problem. Having the information from previous section, one can match the extracted features with corresponding phonemes (classes). Now the task is to define the form of one sample.

Fig. 2.10 goes with the example in Table 2.2. The numbers in the first line are frame indices. The second line contains the known frame labels, where each frame is described by a vector of 40 features.

There is a possibility to take all frames labeled as "a" and consider the corresponding vectors directly as samples. However, as the labeling was not done manually and therefore cannot be considered as 100% correct, we introduce a parameter called `border_size`. Fig. 2.10 shows that we omit the frames on borders with another phoneme label and take only those in the middle.

16	17	18	19	20	21	22	23	24	25	26	27	28	29	30	31	32	33	34
a	a	a	a	a	a	a	a	a	a	n	n	n	n	n	n	o	o	
f <sub>1</sub>	f <sub>1</sub>	f <sub>1</sub>	f <sub>1</sub>	f <sub>1</sub>	f <sub>1</sub>	f <sub>1</sub>	f <sub>1</sub>	f <sub>1</sub>	f <sub>1</sub>	f <sub>1</sub>	f <sub>1</sub>	f <sub>1</sub>	f <sub>1</sub>	f <sub>1</sub>	f <sub>1</sub>	f <sub>1</sub>	f <sub>1</sub>	
.	.	.	.	.	.	.	.	.	.	.	.	.	.	.	.	.	.	
.	.	.	.	.	.	.	.	.	.	.	.	.	.	.	.	.	.	
.	.	.	.	.	.	.	.	.	.	.	.	.	.	.	.	.	.	
f <sub>40</sub>	f <sub>40</sub>	f <sub>40</sub>	f <sub>40</sub>	f <sub>40</sub>	f <sub>40</sub>	f <sub>40</sub>	f <sub>40</sub>	f <sub>40</sub>	f <sub>40</sub>	f <sub>40</sub>	f <sub>40</sub>	f <sub>40</sub>	f <sub>40</sub>	f <sub>40</sub>	f <sub>40</sub>	f <sub>40</sub>	f <sub>40</sub>	
bs = 2								bs = 2		bs = 2						bs = 2		bs = 2

FIGURE 2.10: Forming a sample, illustration of parameter `border_size` (`bs`).

Moreover, in Fig. 2.11 parameter `context_size` is introduced. The idea is to consider not only the information of one frame, but also of its context, into one sample.

16	17	18	19	20	21	22	23	24	25	26	27	28	29	30	31	32	33	34				
a	a	a	a	a	a	a	a	a	n	n	n	n	n	n	n	o	o					
f <sub>1</sub>	f <sub>1</sub>	f <sub>1</sub>	f <sub>1</sub>	f <sub>1</sub>	f <sub>1</sub>	f <sub>1</sub>	f <sub>1</sub>	f <sub>1</sub>	f <sub>1</sub>	f <sub>1</sub>	f <sub>1</sub>	f <sub>1</sub>	f <sub>1</sub>	f <sub>1</sub>	f <sub>1</sub>	f <sub>1</sub>	f <sub>1</sub>					
.	.	.	.	.	.	.	.	.	.	.	.	.	.	.	.	.	.	.				
.	.	.	.	.	.	.	.	.	.	.	.	.	.	.	.	.	.	.				
.	.	.	.	.	.	.	.	.	.	.	.	.	.	.	.	.	.	.				
f <sub>40</sub>	f <sub>40</sub>	f <sub>40</sub>	f <sub>40</sub>	f <sub>40</sub>	f <sub>40</sub>	f <sub>40</sub>	f <sub>40</sub>	f <sub>40</sub>	f <sub>40</sub>	f <sub>40</sub>	f <sub>40</sub>	f <sub>40</sub>	f <sub>40</sub>	f <sub>40</sub>	f <sub>40</sub>	f <sub>40</sub>	f <sub>40</sub>	f <sub>40</sub>				
bs = 2		-2	-1			+1	+2	bs = 2		bs = 2		-1				+1	bs = 2		bs = 2			
one sample (cs = 2)								another sample (cs = 1)														

FIGURE 2.11: Forming a sample, illustration of parameter `context_size` (`cs`).



Based on the chosen context size  $cs$  the previous and subsequent vectors are added one by one and forms one feature vector of length  $40 \cdot (2cs + 1)$ . An example for  $cs = 2$  is illustrated in Fig. 2.12.

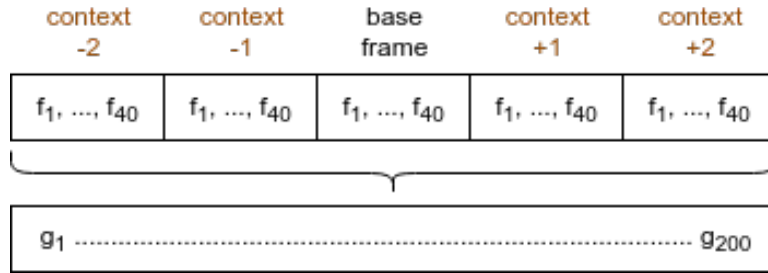


FIGURE 2.12: Example of building a feature vector with context\_size  $cs = 2$ .

Talking about Fig. 2.12, features  $g_1, g_2, \dots, g_{200}$  gives the final feature vector of one sample, which takes the label of the base frame.

The last parameter of the speech dataset generation is the number of samples per class (`n_samples`). The rule of thumb is the more samples the better training results, however, getting best possible training results is not the objective of this work. Therefore we often use less samples to speed up the training process.

To summarize this section, we end up with three parameters of the speech dataset generation process:

- `border_size` (see Fig. 2.10)
- `context_size` (see Fig. 2.11)
- `n_samples` per class

## Splitting data into three disjunctive sets

Fig. 2.13 shows a general approach of data splitting in machine learning. It is used for all classification problems in this work. The training data is used to set up model parameters. Development data is then used for testing during the training process, in order to adjust some learning parameters based on the test results. Finally, a trained model is tested on never-seen testing data. We use splitting: 80% training set; 10% development set; 10% testing set.

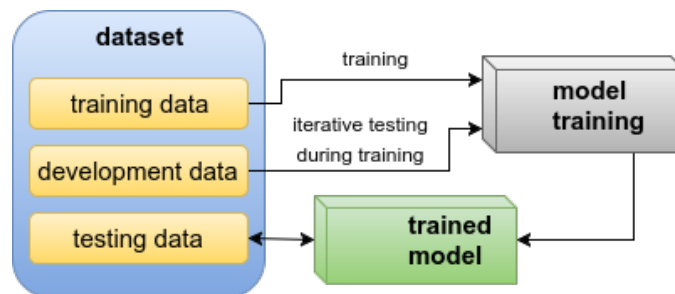


FIGURE 2.13: Using three disjunctive sets of data for a general machine learning process.

## Chapter 3

# Examples

The pruning algorithm is presented on several examples, where each of them has its purpose of being shown. The XOR problem (section 3.1) should verify the ability of finding an optimal network structure. Section 3.2 comes with another 2D problem, where one feature carries more information than the other one. The Rule-plus-Exception problem in section 3.3 deals with a minority of samples that has to be treated by a different net part than rule-based samples. The train problem (section 3.4) is a working example of the feature selection procedure. The MNIST database (section 3.5) is widely used in machine learning and can be regarded as commonly known, hence it is an ideal example to present new methods on. Finally, in section 3.6 the pruning algorithm is analysed on a large dataset of phonemes.

### 3.1 XOR Function

The standard Exclusive OR (XOR) function is defined by truth Table 3.1. Based on this function one can build a classification problem of two features and two classes.

$x_1$	$x_2$	$y$
0	0	0
0	1	1
1	0	1
1	1	0

TABLE 3.1: XOR function.

This problem serves perfectly for a demonstration of network optimization methods, as two optimal architectural solutions producing the XOR function are already known (Fig. 3.1) <sup>1</sup>.

---

<sup>1</sup>The known (e.g. from (Bradley, 2006)) minimal network architectures producing the XOR function  $[2, 2, 1]$  and  $[2, 3, 1]$  are adjusted to  $[2, 2, 2]$  and  $[2, 3, 2]$  in Fig. 3.1 in order to comply with the conventions introduced in chapter 2. The number of output neurons always equals the number of classes. The number of hidden-output synapses might not be optimized in this study.

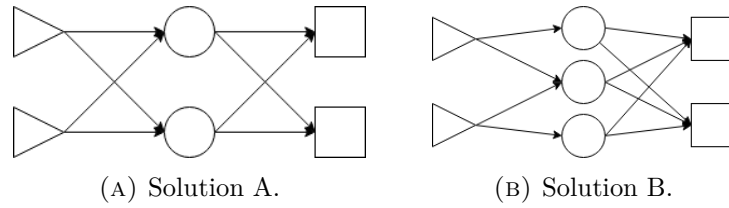


FIGURE 3.1: Optimal network architectures producing the XOR function.

With this knowledge we can prove that the pruning algorithm is (or is not) able to find the optimal solution. If the method is correct, it should end up with one of the shown architectures (Fig. 3.1a or Fig. 3.1b).

The truth Table 3.1 ruled the generation of a 2D dataset illustrated in Fig. 3.2. The two classes can be linearly separated by two lines (corresponding to two neurons, see Fig. 3.1a) and each class consists of 1000 samples. Each sample was randomly assigned to one of the two possible points belonging to its class (e.g. (0,0) or (1,1) for class 0) and then randomly placed in the surrounding area within a specified range ( $r = \frac{\sqrt{2}}{4}$ ).

The samples of each class were then splitted into three sets in the following manner: 80% to a training set, 10% to a validation set and 10% to a testing set.

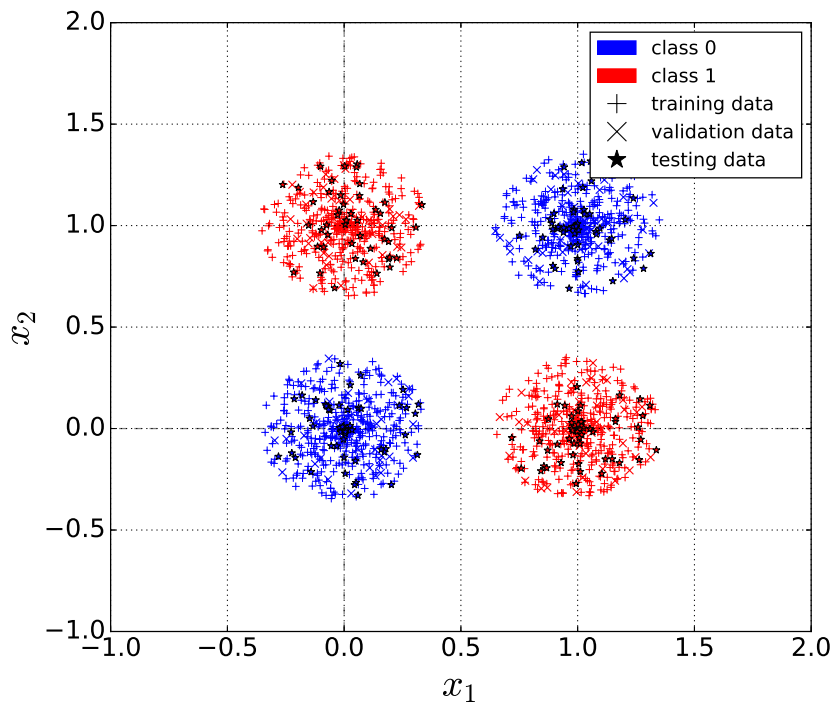


FIGURE 3.2: The XOR dataset.

The goal of this example is to show that the pruning algorithm finds one of the known minimal network structures (Fig. 3.1). An oversized network  $[2, 50, 2]$  is used as the starting point. The following Table 3.2 shows all the experiment settings.

<i>initial network</i>		<i>learning parameters</i>		<i>pruning parameters</i>	
structure	[2, 50, 2]	learning rate	0.3	required accuracy	1.0
n synapses	200	number of epochs	50	retrain	True
transfer fcn	sigmoid	minibatch size	1	retraining epochs	50

TABLE 3.2: Experiment settings for the XOR example.

### Results: XOR Function

Fig. 3.3 describes the pruning process. We can see the number of synapses, the network structure and the classification accuracy for single pruning steps (see [PA]). When the required accuracy (1.0) was not reached, the corresponding steps are transparent in the figure, indicating they were forgotten.

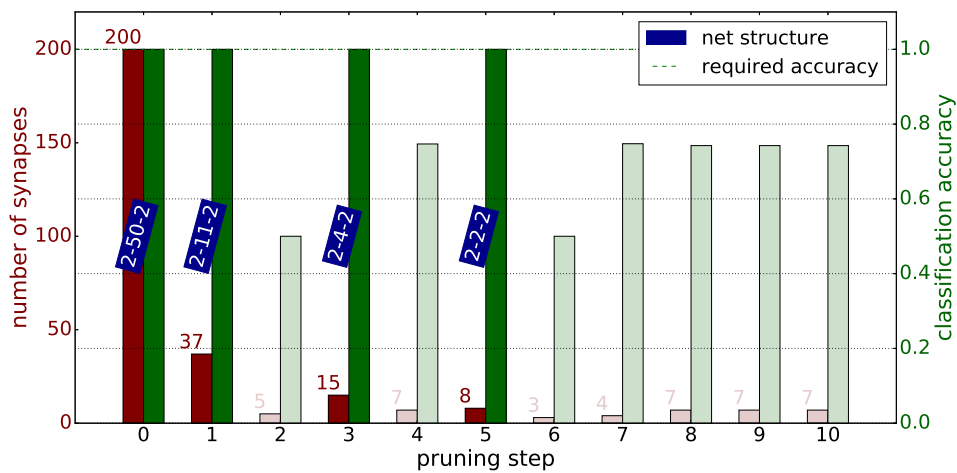


FIGURE 3.3: Illustration of the pruning procedure applied on XOR dataset (selected observation).

In Fig. 3.4 the hypothesis of this experiment is confirmed. We ran 100 observations of the experiment. In Fig. 3.4a we can see that in 47 out of 100 cases the pruning algorithm changed the network to [2, 2, 2] architecture (Fig. 3.1a), in 45% of the cases it resulted with [2, 3, 2] (Fig. 3.1b) and only in 8% it failed to find the optimal architecture. Fig. 3.4b gives statistics for the final number of synapses in these three cases.

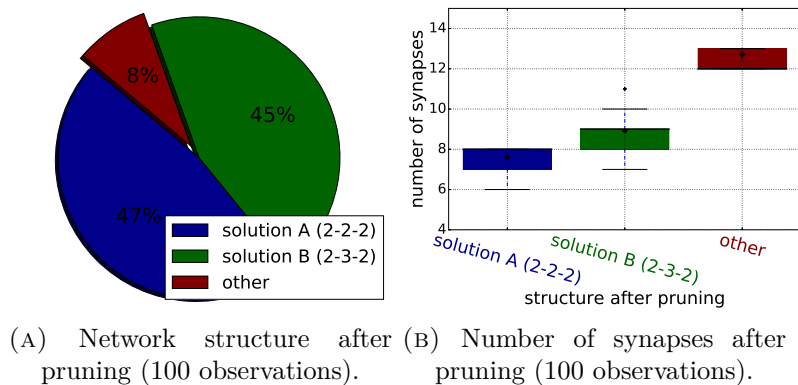


FIGURE 3.4: Pruning results for XOR dataset.

### 3.2 Unbalanced Feature Information

This example is adopted from (Karnin, 1990). The problem is again two-dimensional having two non-overlapping classes as depicted in Fig. 3.5. The samples are uniformly distributed in  $[-1, 1] \times [-1, 1]$  and the classes are equally probable, separated by two lines in 2D space ( $x_1 = a$  and  $x_2 = b$ , where  $a = 0.1$  and  $b = \frac{2}{a+1} - 1 \approx 0.82$ ). Clearly, the problem can be solved by two neurons, similarly as the previous one.

What is interesting about this two-classes layout is that feature  $x_1$  is much more important for the global classification accuracy than feature  $x_2$ . Having  $x_1$  information, based on Fig. 3.5 one could potentially classify more than 90% of the samples. Opposite of that, we cannot say much with information from feature  $x_2$  only. And this is something that also the pruning algorithm should find out.

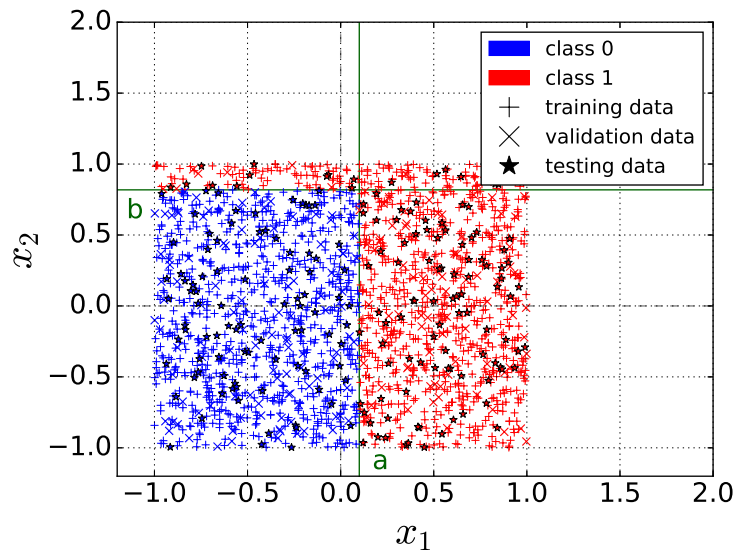


FIGURE 3.5: The UFI dataset.

Hence, we focus on synapses connecting the input and the hidden layer (shortly input-hidden synapses). We know the required network structure is  $[2, 2, 2]$ , as two lines are needed to separate the data in 2D space. Actually, we even know the lines must be parallel to coordinate axes, which means that each of the hidden units needs one of the features only. Therefore, the first hypothesis here is that pruning of input-hidden synapses should result in one of the cases in Fig. 3.6.

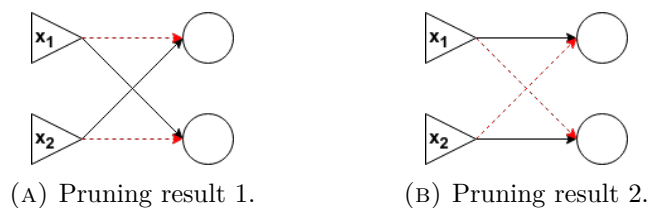


FIGURE 3.6: Expected pruning of input-hidden synapses (UFI problem).

To prove this behaviour, we ran an experiment with settings in Table 3.3.

<i>initial network</i>		<i>learning parameters</i>		<i>pruning parameters</i>	
structure	[2, 2, 2]	learning rate	0.7	required accuracy	0.98
n synapses	8	number of epochs	50	retrain	True
transfer fcn	sigmoid	minibatch size	1	retraining epochs	50

TABLE 3.3: Experiment settings for the UFI example.

The second hypothesis is that the synapse connected to the first feature ( $x_1$ ) is more important and therefore, the other synapse (the one connected to feature  $x_2$ ) should always be removed first.

### Results: Unbalanced Feature Information

In Fig. 3.7 the first hypothesis is confirmed. We ran the experiment 100 times. In 48 cases, the pruning of input-hidden synapses finished with the result shown in Fig. 3.6a and it finished with the result shown in Fig. 3.6b in 44% of the cases.

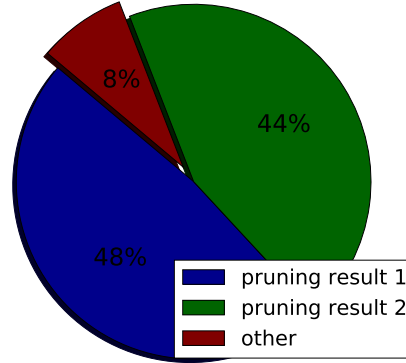


FIGURE 3.7: Results of pruning (see Fig. 3.6) input-hidden synapses (100 observations, UFI example).

In other words, with a probability of 92% the algorithm is able to find the axis-parallel lines and reveals that each of the lines needs the information from corresponding feature only. In the remaining 8% of the cases the pruning resulted with more than two input-hidden synapses.

The second hypothesis is confirmed in Fig. 3.8. The synapses's significance factor was always (100 observations) greater for the synapse coming from feature  $x_1$  than for the synapse connected to  $x_2$ . By definition (see [PA]), the pruning method eliminates the synapses with low significance factors first, therefore the information coming from feature  $x_1$  would live longer in the network than the  $x_2$  information.

Let's try to explain this result. Consider  $w_{r1}$  to be the weight of the synapse connecting the  $x_1$  feature and  $r^{th}$  hidden neuron (with bias  $b_r$ ) and  $w_{s2}$  to be the weight of the synapse coming from feature  $x_2$  to  $s^{th}$  hidden neuron (with bias  $b_s$ ), then by neuron definition (Rosenblatt, 1958) we created two

lines, perpendicular one to each other, as follows.

$$w_{r1} \cdot x_1 + 0 \cdot x_2 + b_r = 0 \quad (3.1)$$

$$x_1 = -\frac{b_r}{w_{r1}} \quad (3.2)$$

$$0 \cdot x_1 + w_{s2} \cdot x_2 + b_s = 0 \quad (3.3)$$

$$x_2 = -\frac{b_s}{w_{s2}} \quad (3.4)$$

In Fig. 3.5 we see that  $a < b$ . To generalize the problem (assuming normalised feature vectors, see chapter 2) we state  $|a| < |b|$ , meaning we want:

$$\left| -\frac{b_r}{w_{r1}} \right| < \left| -\frac{b_s}{w_{s2}} \right| \quad (3.5)$$

Hence we expect:

$$|w_{r1}| > |w_{s2}| \quad (3.6)$$

Out of this we expect a weight magnitude to be greater for more important synapses.

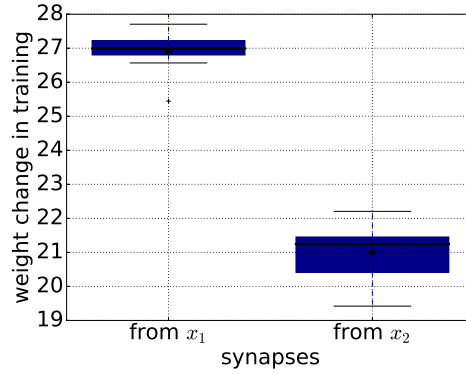


FIGURE 3.8: Weight change in training for the remaining input-hidden synapses (100 observations).

The weight magnitude seems to be a perfect measure to find feature significance factor. However, as we do not use a weight decay (see the learning approach in chapter 2), in general the more epochs we learn the greater weight magnitudes we get. Therefore small initial weight values do not affect the result significantly and so we can state:

$$|w_{ji}(t)| \approx |w_{ji}(t) - w_{ji}(0)| \quad (3.7)$$

where  $w_{ji}(0) \in N(0, 1)$  is the initial value of weight  $w_{ji}$  and  $t$  is time. Summing it up we can say that the `kitt` measure [ref] based on weight change is equally good as the magnitude measure assuming enough training epochs (e.g. 50).

### 3.3 Rule-plus-Exception

This four-dimensional problem is originally adopted from (Mozier and Smolensky, 1989) and is also used in (Karnin, 1990). The task is to learn another Boolean function:  $AB + \overline{A}\overline{B}\overline{C}\overline{D}$ . A single function output should be on (i.e. equals 1) when both  $A$  and  $B$  are on, which is the *rule*, and it should also be on when the *exception*  $\overline{A}\overline{B}\overline{C}\overline{D}$  occurs.

Clearly, the *rule* occurs more often than the *exception*, therefore the samples corresponding with the *rule* should be more important for the global classification accuracy. The hypothesis is that the pruning method should suggest the part of network, which deals with the *exception*, to be eliminated first - before network elements dealing with the *rule*.

To test this hypothesis, a dataset of 10000 samples was generated. Each sample consists of four features:  $[a, b, c, d]$ . Each of these features (for every sample) was randomly set to be *on* (1) or *off* (0). Then, whenever the *rule* occurred ( $a = 1 \wedge b = 1$ ), the sample was assigned to class 1 (as a *rule* sample). If the *exception* occurred ( $a = 0 \wedge b = 0 \wedge c = 0 \wedge d = 0$ ), the sample was also labeled as 1 (as an *exception* sample). Otherwise, the sample was assigned to class 0. Thereby the generated dataset consisted of:

- 2511 *rule* samples (class 1);
- 649 *exception* samples (class 1);
- 6840 samples in class 0.

The function is expected to be learned by two hidden neurons, one dealing with the *rule* and the other one with the *exception*. We focus on input-hidden synapses again. Two possible expected pruning results are shown in Fig. 3.9.

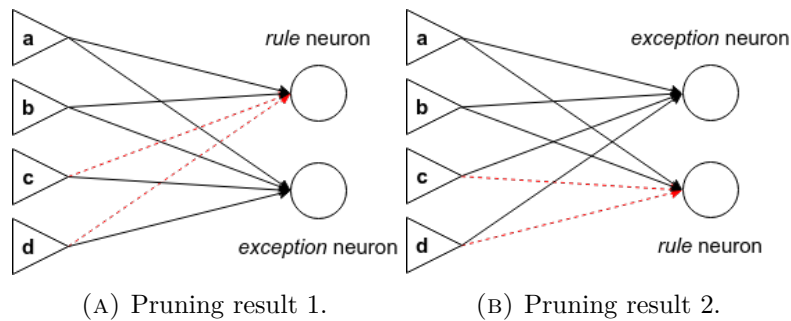


FIGURE 3.9: Expected pruning of input-hidden synapses (RPE problem).

We ran the learning-pruning procedure with the settings listed in Table 3.4.

initial network		learning parameters		pruning parameters	
structure	[2, 2, 2]	learning rate	1.0	required accuracy	1.0
n synapses	8	number of epochs	50	retrain	True
transfer fcn	sigmoid	minibatch size	1	retraining epochs	50

TABLE 3.4: Experiment settings for the RPE example.



### Results: Rule-plus-Exception

Fig. 3.10 supports the hypothesis that one hidden neuron forms the *rule* and the other one the *exception*. With a probability of 97% the pruning finished with one of the structures in Fig. 3.9.

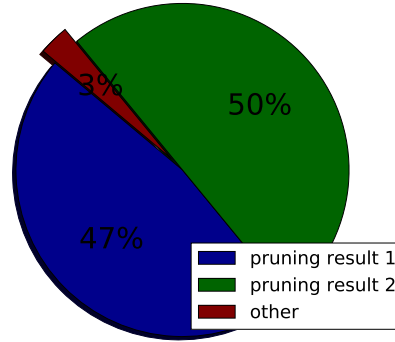


FIGURE 3.10: Results of pruning (see Fig. 3.9) input-hidden synapses (100 observations, RPE example).

The same thing is confirmed by Fig. 3.11. It shows weight change in training (kitt significance factor) for all 8 input-hidden synapses. We can see that synapses connecting the *rule* neuron with feature *c* ( $s_{rc}$ ) and feature *d* ( $s_{rd}$ ) were suggested as least important (resulted in structures in Fig. 3.9).

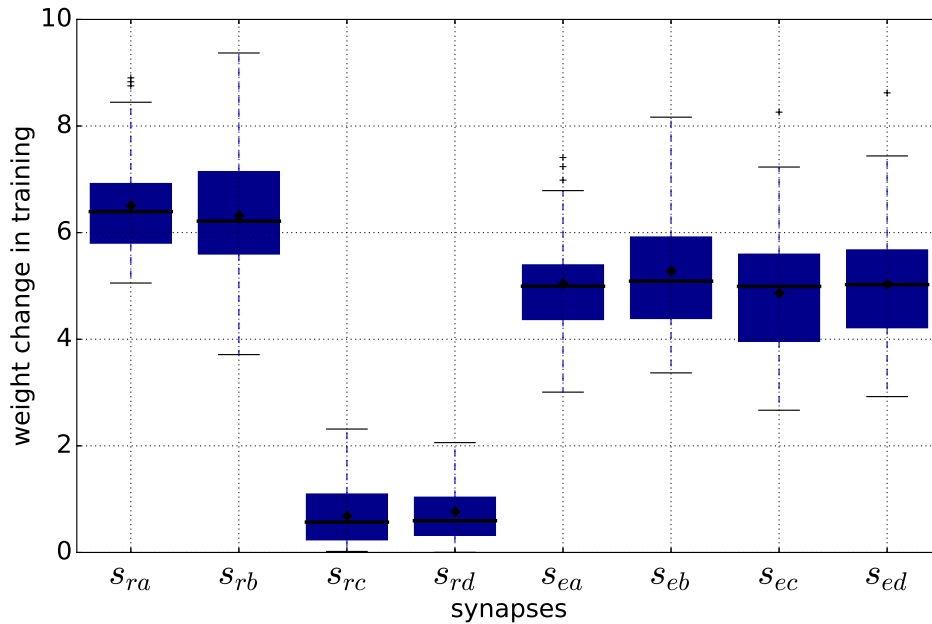


FIGURE 3.11: Weight change in training for input-hidden synapses (100 observations, RPE example).

Additionally, synapses responsible for *rule* ( $s_{ra}$  and  $s_{rb}$ ) have a greater mean significance than the synapses connected with the *exception* neuron ( $s_{e*}$ ).

### 3.4 Michalski's Trains

The train problem was originally introduced in (Larson and Michalski, 1977). The task was to determine concise decision rules distinguishing between two sets of trains (Eastbound and Westbound). In (Mozer and Smolensky, 1989), they presented a simplified version illustrated in Fig. 3.12.

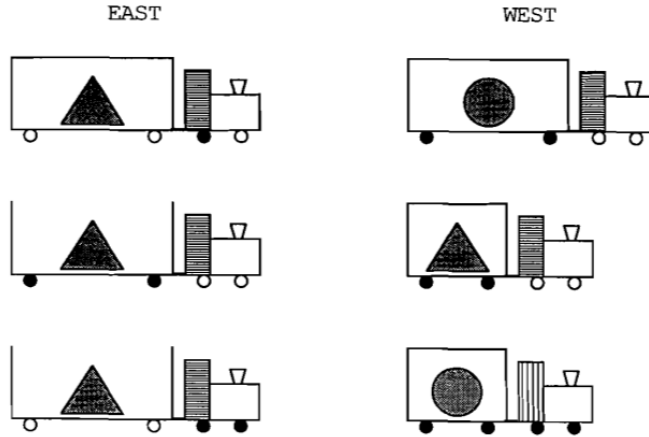


FIGURE 3.12: Michalski's train problem.

Each train is described by 7 binary features listed in Table 3.5.

	feature	encoded as 0	encoded as 1
0	car length	long	short
1	car type	open	closed
2	cabin pattern	vertical lines	horizontal lines
3	load shape	triangle	circle
4	color of trailer wheels	white	black
5	color of first car wheel	white	black
6	color of second car wheel	white	black

TABLE 3.5: Features describing a train.

Having Table 3.5 we can encode the trains shown in Fig. 3.12 into feature vectors as follows in Table 3.6.

<i>class EAST</i>		<i>class WEST</i>	
east 1	$[0, 1, 1, 0, 0, 0, 1]^T$	west 1	$[0, 1, 1, 1, 1, 0, 0]^T$
east 2	$[0, 0, 1, 0, 1, 0, 0]^T$	west 2	$[1, 1, 1, 0, 1, 0, 0]^T$
east 3	$[0, 0, 1, 0, 0, 1, 1]^T$	west 3	$[1, 1, 0, 1, 1, 1, 1]^T$

TABLE 3.6: Feature vectors for different train types.

The task is to determine the minimal number of input features capable of the east-west classification based on the six possible types in Table 3.6 (or in Fig. 3.12).

The hypothesis is that the pruning algorithm should select the needed features by eliminating unimportant input-hidden synapses. Looking at Fig. 3.12 one of the solutions could be keeping features (0, 3), because the shape of the load together with the length of the car is enough to distinguish *west* trains from *east* trains. Another solution, for example, is keeping the car length, car type and color of the second car wheel - features (0, 1, 6).

To test our pruning algorithm on this feature selection task, a dataset of 6000 samples (3000 west and 3000 east trains) was generated. The three possible train types for each class (Fig. 3.12) are equally distributed among the samples, meaning we have 1000 samples of each train type.

As shown in (Mozer and Smolensky, 1989), one hidden neuron is enough to learn this problem, hence we started with the network structure [7, 1, 2]. The experiment parameters are listed in Table 3.7.

<i>initial network</i>		<i>learning parameters</i>		<i>pruning parameters</i>	
structure	[7, 1, 2]	learning rate	0.3	required accuracy	1.0
n synapses	9	number of epochs	100	retrain	True
transfer fcn	sigmoid	minibatch size	1	retraining epochs	10

TABLE 3.7: Experiment settings for the train example.

We ran 100 observations of the experiment and considered the features that were not cut out, as a result of a single experiment.

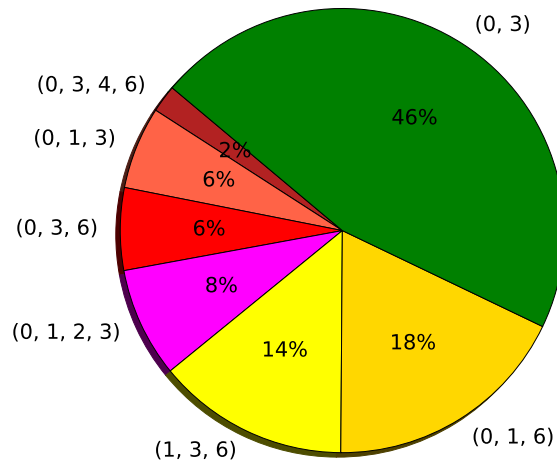


FIGURE 3.13: Results of feature selection by the pruning algorithm (train example). The labels corresponds with feature indices in Table 3.5.

The result pie in Fig. 3.13 shows that the pruning algorithm found the best possible solution ((0, 3) - the car length and the load shape) in 46% of the cases. We can regard the (0, 1, 6) and (1, 3, 6) as another (not best but also good) solutions. The rest we consider as fail cases, as all of them include features (0, 3) and the other features are redundant. To sum it up, we got a perfect solution: 46%; a good solution: 32%; a bad solution: 22%.

### 3.5 Handwritten Digits (MNIST)

The MNIST (Modified National Institute of Standards and Technology) database (Wikipedia, 2004) is a large database of handwritten digits that is widely used for training and testing methods in the field of machine learning.

The dataset was downloaded from (LeCun and Cortes, 1998). Some of the digits were written by employees of American Census Bureau (*United States Census Bureau* 2017) and some by students of an American high school. In total 70000 samples were collected. Examples are shown in Fig. 3.14.

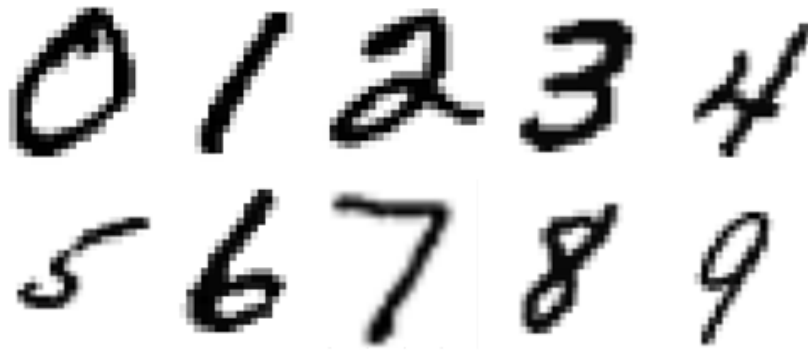


FIGURE 3.14: Examples of MNIST dataset.

Each sample is a grayscale image (normalised to  $[0, 1]$ ) of size  $28 \times 28$  pixels. This gives row-by-row a vector of 784 features. The data was splitted into a training set of 50000 samples, a validation set of 10000 samples and a testing set of 10000 samples.

From (LeCun and Cortes, 1998) we know the problem can be learnt by a feedforward network with one hidden layer up to high accuracy (98 – 99%). The first task is to achieve similar results with the implemented neural net framework. We tested the following learning settings (Table 3.8).

<i>network parameters</i>		<i>learning parameters</i>	
structure	[784, 20, 10]	learning rate	0.3
n synapses	15880	number of epochs	100
transfer function	sigmoid	batch size	10

TABLE 3.8: Settings for training a dense feedforward net on the MNIST dataset.

The training results are summarized in Table 3.9. A confusion matrix for the testing data is given in Fig. 3.15.

	<i>accuracy</i>	<i>MSE</i>
<i>training data</i>	97.2%	0.526
<i>testing data</i>	94.3%	1.025

TABLE 3.9: Training results on MNIST dataset.

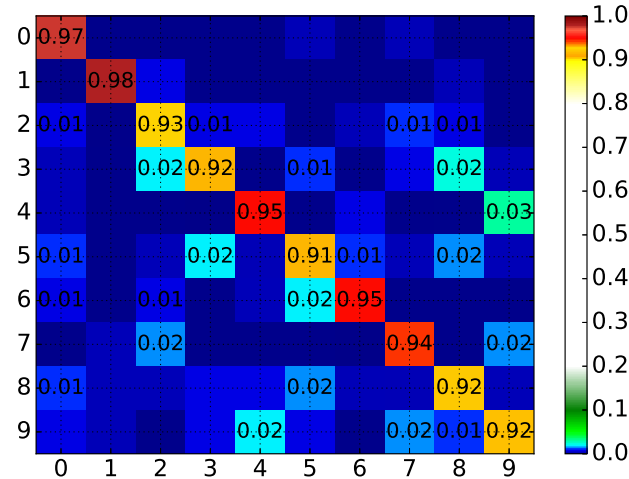


FIGURE 3.15: Confusion matrix (MNIST, testing data).

In the following, the pruning method is analysed on networks trained on the MNIST database. Parameters of the learning-pruning procedure are listed in Table 3.10.

<i>initial network</i>		<i>learning parameters</i>		<i>pruning parameters</i>	
structure	[784, 20, 10]	learning rate	0.3	required accuracy	0.97
n synapses	15800	number of epochs	30	retrain	True
transfer fcn	sigmoid	minibatch size	10	retraining epochs	10

TABLE 3.10: Experiment settings for the MNIST example.

The hypothesis is that the initial number of synapses in the network (15800) is redundant, as well as the number of features (784). In Fig. 3.16 we can see a selected observation of the pruning process. The number of synapses was reduced to 1259 and the number of used features to 465, while the classification accuracy was kept on 97%. The pruning procedure finished in 424 pruning steps (explained in [PA]).

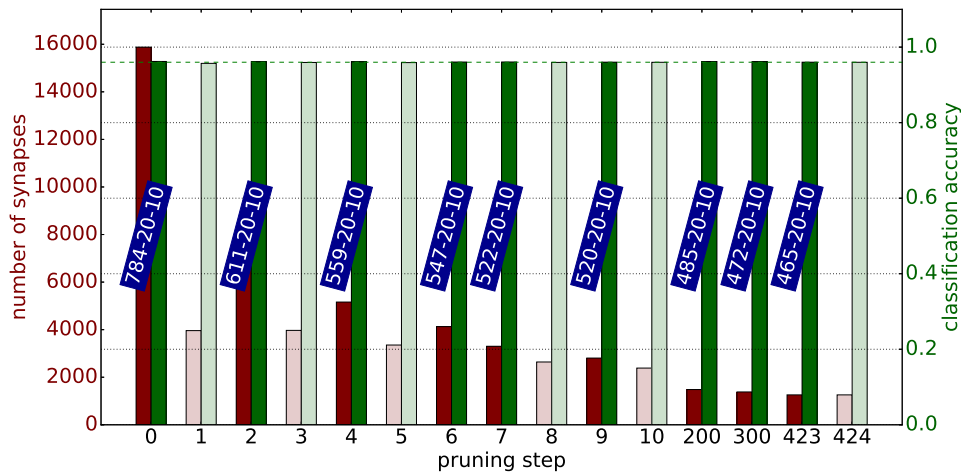


FIGURE 3.16: Illustration of the pruning procedure applied on MNIST dataset (selected observation). Required accuracy: 97%.

In Fig. 3.17, we can see a comparison of the evaluation time. We compare a fully-connected (initial) network to a pruned one. Bars are given for the three data groups (training: 50000 samples, validation: 10000 samples, testing: 10000 samples). The processing time was reduced by nearly half after the pruning, which led to a reduction of weight matrix dimension (see [SHRINK]).

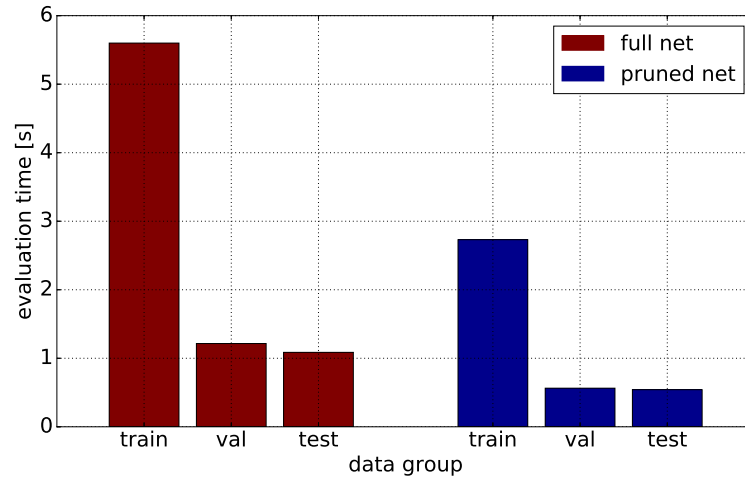


FIGURE 3.17: Evaluation (accuracy and error computation) time for all data groups (pruned vs. full net).

Fig. 3.18 gives the statistics by running 10 observations of the pruning procedure for several values of required classification accuracy. We observed the number of synapses (red axis) and used features after pruning (blue axis).

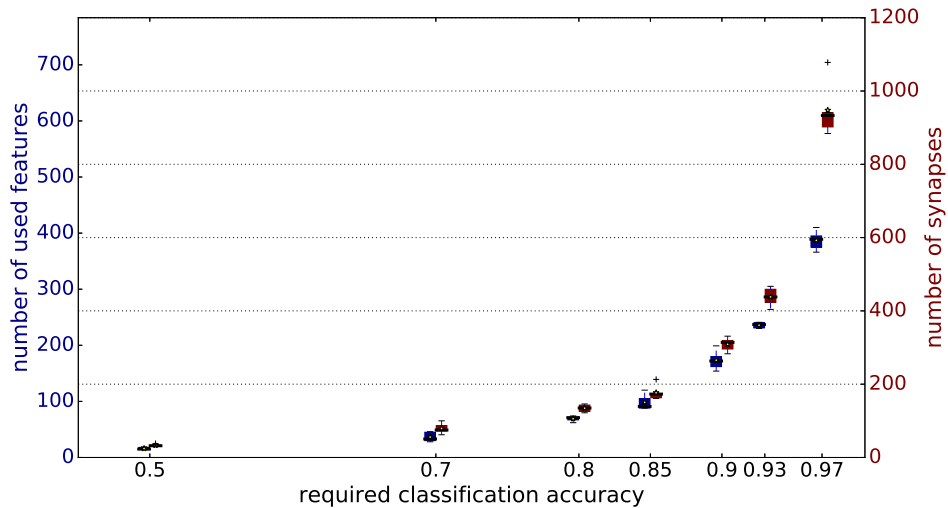


FIGURE 3.18: Minimal number of features and synapses to get required classification accuracy (MNIST data).

The results show that *less than a tenth* of the synapses and *about a half* of the features are needed to keep the maximal classification accuracy (97%). It is also worth saying that the MNIST dataset can be learnt to 50% using only 20 features and a network with 38 synapses. In the following, these two results are further analysed.

### Minimal MNIST network

At first, we focus on a pruned network capable of MNIST classification with accuracy of 50% (Fig. 3.19). This example is simple enough to show the feature selection method described in [ref FS].

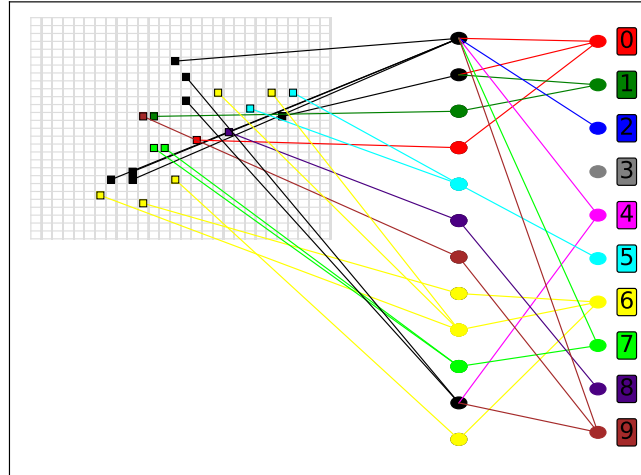


FIGURE 3.19: Result of network pruning and path tracking, MNIST data, accuracy: 50%.

Each class (digit in this case) has its color. If a hidden unit has one output connection only, it inherits the color of the class it is connected to. The features (pixels of the  $28 \times 28$  image) are then colored in the same way. If a hidden unit influences more than one class, it is blacked. All features connected to a black hidden unit are then blacked as well, as they also affects more than one class.

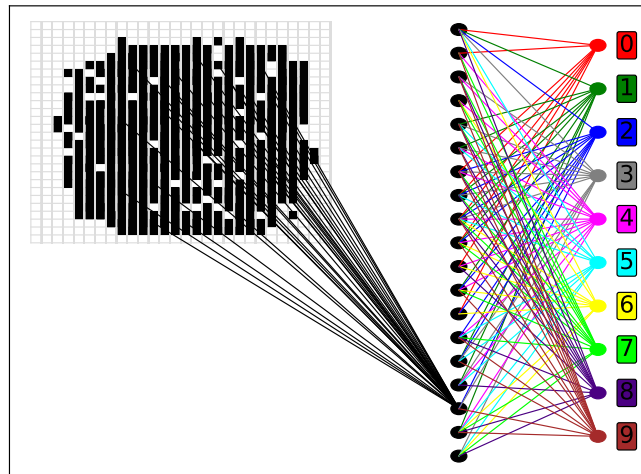


FIGURE 3.20: Result of network pruning and path tracking (shown 17<sup>th</sup> hidden neuron only), MNIST data, accuracy: 97%.

A pruned network capable of 97% accurate classification is visualized in Fig. 3.20. To make the figure clearer, only synapses coming to the 17<sup>th</sup> hidden unit are drawn between the input and hidden layer.

We can see that each of the features affects more than one class in this case. Therefore we better use the visualization in Fig. 3.21.

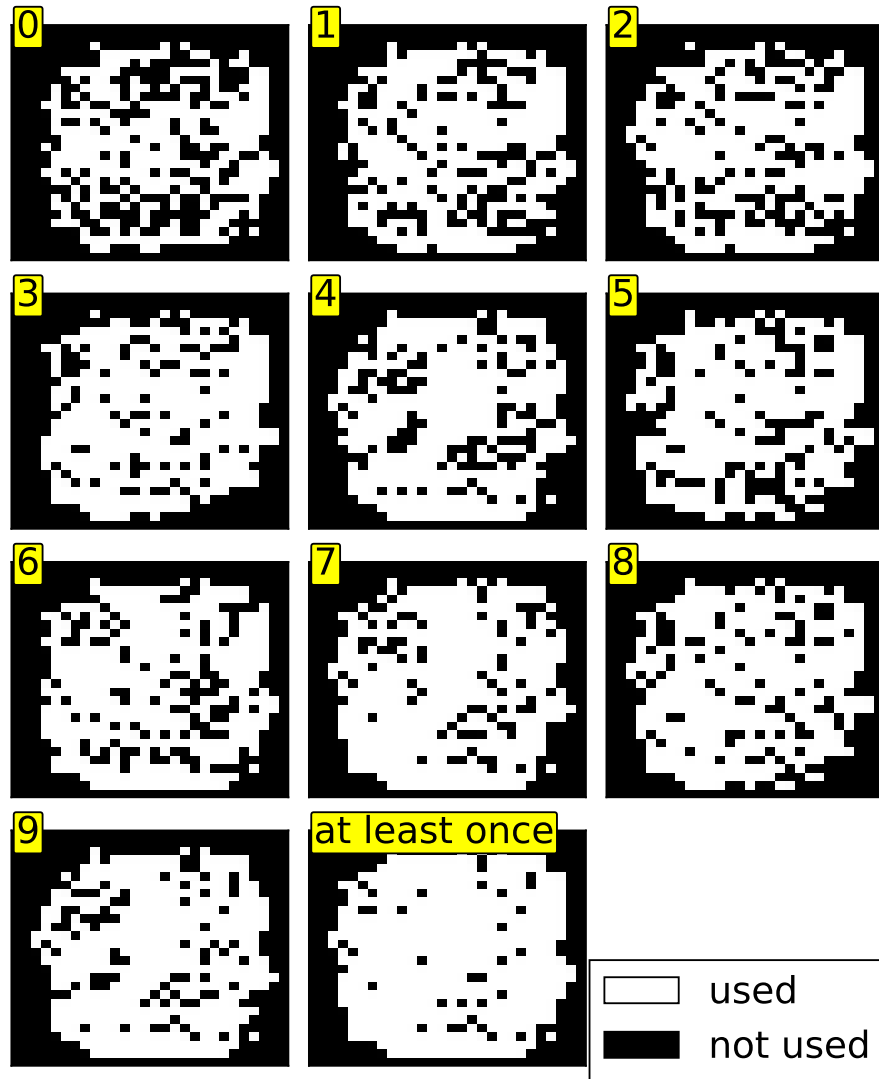


FIGURE 3.21: Used features for individual classes, MNIST data, accuracy: 97%.

Knowing all the remaining synapses are important for classification, we can track the paths from individual classes to features. This way we distinguish features connected to a selected class from those that do not affect that class. Fig. 3.21 shows important features for each class (digit) separately. Note that the *at-least-once* subplot corresponds to the features shown in Fig. 3.20. It shows all features used by at least one class.

Some more ideas about path tracking in pruned networks are further discussed in section 4.3.



### 3.6 Phonemes (Speech Data)

The process of speech data gathering is described in section 2.4. The dataset generation process has three parameters: `border_size` ( $bs$ ), `context_size` ( $cs$ ) and `n_samples` ( $ns$ ).

In this example, we first try to find optimal parameter settings, which would lead to a maximal trainability. The general rule is the more samples the better trainability, therefore we fix  $ns = 1000$  and determine the other parameters at first. See Table A1.1 for details of all generated datasets differing in  $bs$  and  $cs$ . It reveals that phoneme "F" does not have enough occurrences (less than  $ns = 1000$ ) in the data, and of course the number of occurrences decreases with growing  $bs$ . For  $bs \geq 6$  even more phonemes ("D", "F", "N", "Q", "R", "T") have less than 1000 occurrences.

Table 3.11 shows the experiment settings.

experiment settings		learning parameters	
n observations	5	learning rate	0.1
observed value	MSE' (Eq. (2.19))	n epochs	50
network structure	$[40 \cdot (2cs + 1), 50, 40]$	batch size	10

TABLE 3.11: Speech dataset: experiment settings for determination of optimal  $bs$  and  $cs$ .

We ran 5 observations of a simple network training for every combination of  $bs \in [0, 5]$  and  $cs \in [0, 9]$ . Fig. 3.22 shows average MSE' (see Eq. (2.19)) values. Complete results can be tracked in Table A1.2.

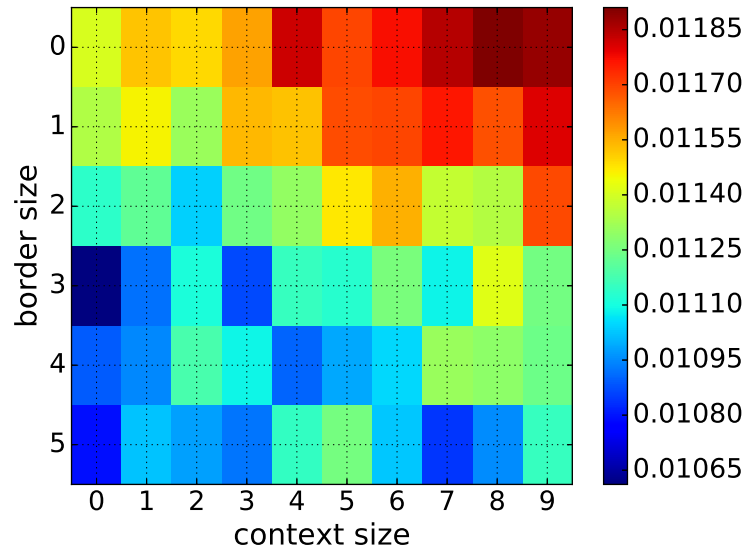


FIGURE 3.22: Test MSE' (Eq. (2.19)) for various parameters  $bs$  and  $cs$  ( $ns = 1000$ , 5 observations, see Table A1.1).

The experiment result says that a bigger `context_size` ( $cs > 2$ ) does not go well together with a low `border_size` ( $bs \leq 2$ ). We can state that the `border_size` should better be greater than two. Then the `context_size`

does not influence the trainability much. We must keep in mind that the experiment is too simple to give a reliable estimate (simple network structure, few training epochs), however, it gives an initial idea of a general trend, which is enough for the purposes of this work. For the experiments below we consider this settings:

- border\_size:  $bs = 3$
- context\_size:  $cs = 3$
- n\_samples:  $ns = 10000$

### Analysis of the Generated Speech Dataset

The goal of this section is to show what kind of data we actually work with. In Fig. 3.23 we can see one randomly selected sample for each phoneme. For a more illustrative view the context is cut out ( $cs = 0$ ), hence we see 40 features corresponding to 40 frequency filters (see Fig. 2.9).

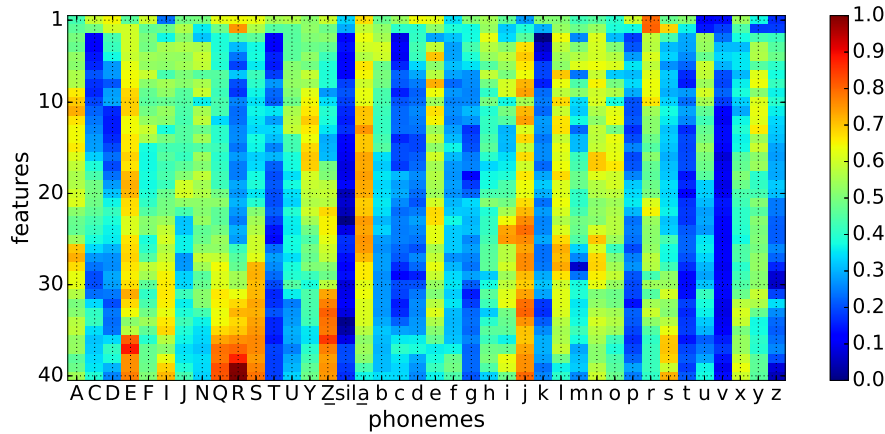


FIGURE 3.23: Randomly selected sample for each phoneme,  $cs = 0$ .

Fig. 3.24 shows an average feature vector out of 10000 samples for each phoneme. Here we can find some patterns.

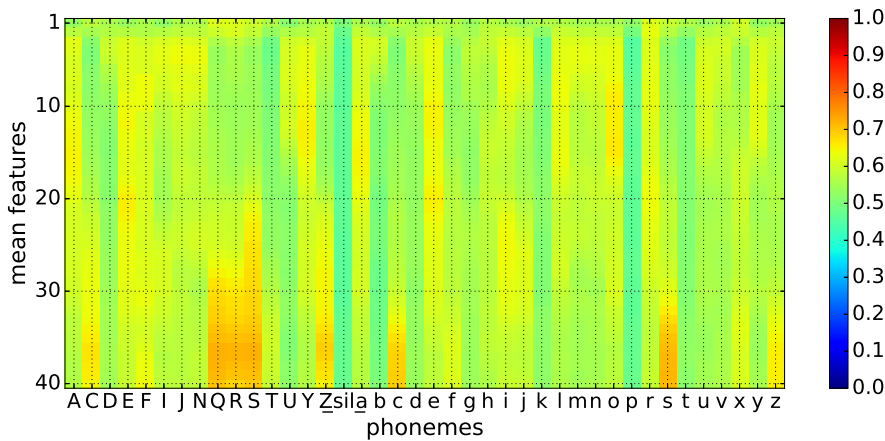


FIGURE 3.24: Average sample for each phoneme,  $cs = 0$ .

For example, the pause ("sil") is very similar to phoneme "p" having low values for all frequencies. Phonemes "A" and "a" also take a similar course, as well as high-frequency groups ("Q", "R", "S") or ("c", "s", "z").

Using the derived parameter settings ( $cs = 3$ ) we end up with a feature vector of length 280. An example for each class is shown in Fig. 3.25. Average values can be found in appendix A1, Fig. A1.1.

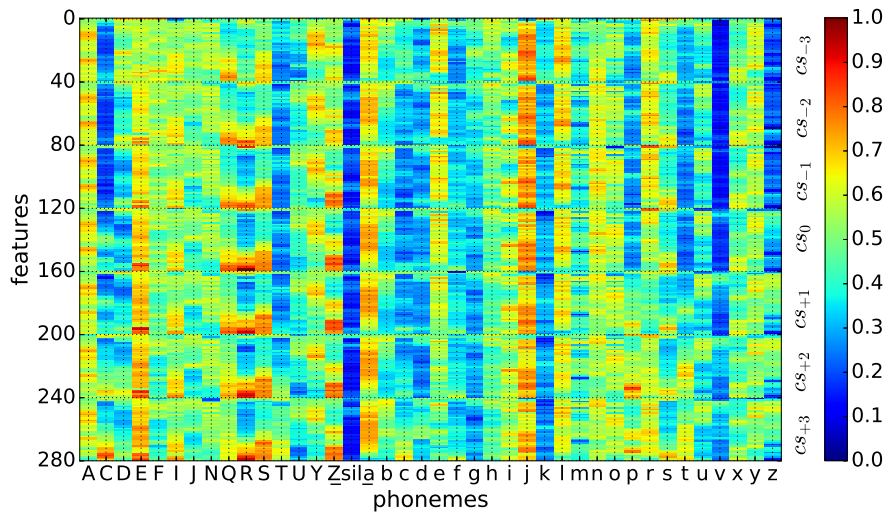


FIGURE 3.25: Randomly selected sample for each phoneme,  $cs = 3$ .

## Classification Results: Speech Dataset

At first we must keep in mind that getting the best possible classification accuracy is not the goal in this work. Rather than spending months of computation time for training huge networks, we choose a simpler network structure and try to get the best out of it. Two different network structures were trained:

1. Network  $[280, 50, 2, 50, 40]$  (bottleneck<sup>2</sup> network);
2. Network  $[280, 100, 50, 40]$ .

The learning parameters for both networks are listed in Table 3.12.

dataset		learning parameters	
n samples / class	5000	learning rate	0.07
border size	3	n epochs	100
context size	3	batch size	10

TABLE 3.12: Phonemes: dataset and learning parameters.

<sup>2</sup>A bottleneck network contains a layer that consists of few nodes compared to the previous layers. It can be used to get a representation of the network input with reduced dimensionality.

### 1. Network (bottleneck)

The network with the bottleneck layer was trained to test accuracy 30% ( $MSE' = 0.0105$ ). A complete confusion matrix can be found in appendix A1, Fig. A1.2. The confusion matrix helped us find phonemes that had been trained better compared to the others. We focused on phonemes with recall<sup>3</sup> greater than 0.5.

The purpose of training a bottleneck network is the reduction of input's dimensionality. Using a layer with just two neurons usually does not lead to a high classification accuracy (also confirmed here), but the advantage is that it can be illustrated in 2D space.

For the selected phonemes, Fig. 3.26 shows the representation of testing samples in the bottleneck layer. We used the *Sigmoid* transfer function, so all samples lie in  $[0, 1] \times [0, 1]$ .

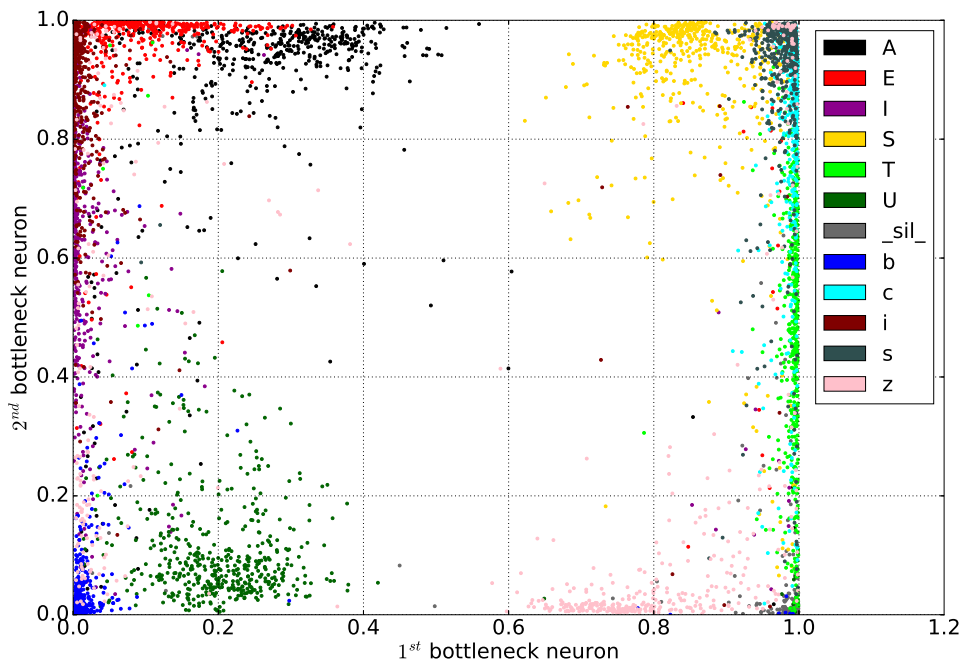


FIGURE 3.26: Representation of individual phonemes in the 2D bottleneck layer (selected phonemes).

The figure confirms some intuitive expectations. For example, samples of phoneme "I" are close to representations of phoneme "i" and also not far away from "A" and "E" samples. Another area contains samples of "S" together with "s" and "c" samples.

The bottleneck network with two neurons is a simple example of how the work in networks can be illustrated.

<sup>3</sup>Recall score is the ability of a classifier to find all the positive samples. It is defined as  $\frac{tp}{tp+fn}$ , where  $tp$  is the number of true positives and  $fn$  the number of false negatives.

## 2. Network

The second network with structure  $[280, 100, 50, 40]$  was trained with the same settings (Table 3.12). The learning ended with accuracy 63.8% and  $MSE' = 0.0063$ . Fig. 3.27 shows the complete confusion matrix.

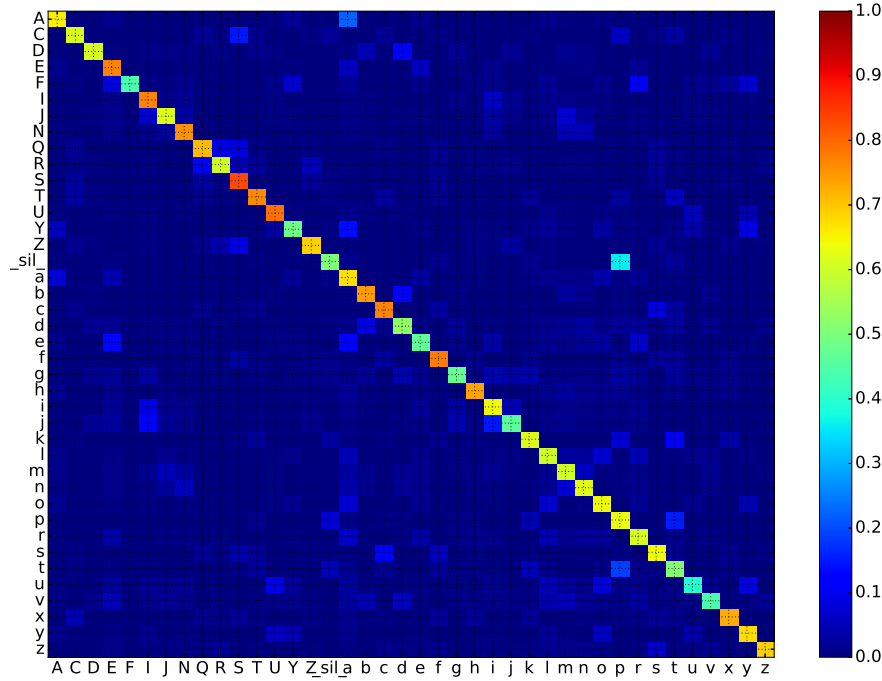


FIGURE 3.27: Confusion matrix of the classification results on the speech dataset.

## Pruning Results: Speech Dataset

The second network ( $[280, 100, 50, 40]$ ) was pruned. In this case we sacrificed a few percent of classification accuracy and required  $req\_acc = 50\%$  only. The pruning process is tracked in Fig. 3.28.

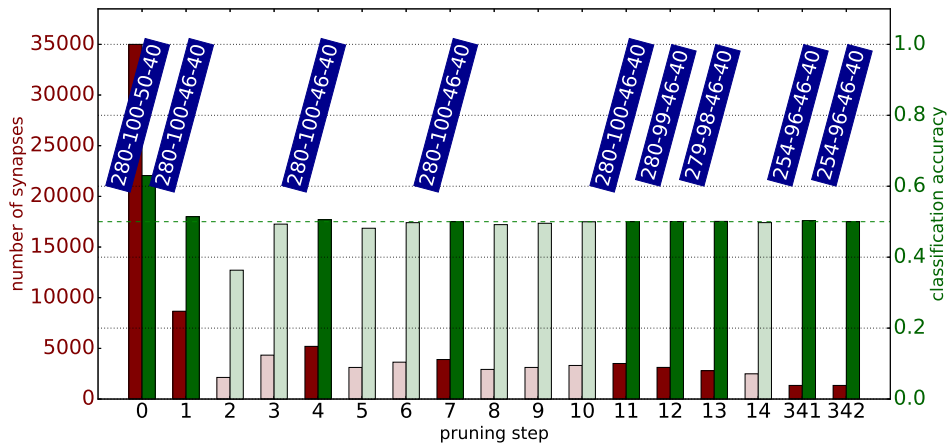


FIGURE 3.28: Illustration of the pruning procedure applied on SPEECH dataset (selected observation). Required accuracy: 50%.

The initial number of synapses 35000 was reduced to 1344. Eight hidden neurons (four in each hidden layer) were cut out. Regarding the input layer 26 neurons were cut out, which reveals that only 254 out of 280 features are necessary to obtain the classification accuracy of 50% on validation data.

The dimensionality reduction is not that significant for this example compared to the others (e.g. MNIST). Also we require a low classification accuracy. However, one must remember that we work with a 40-class problem, which is far from trivial. In the following section we try to find some patterns in the results, which could demystify what is going on in the network.

### **Feature Selection and Pathing: Speech Dataset**

## Chapter 4

# Discussion

Discussion text...

### 4.1 Methods Recapitulation

Methods recapitulation text...

### 4.2 Comparison of Pruning Methods

Comparison of results text...

Random

Magnitude

Karnin

OBD

Kitt

accuracy, convergence time, computation time, number of synapses/features  
(viz Tomas)

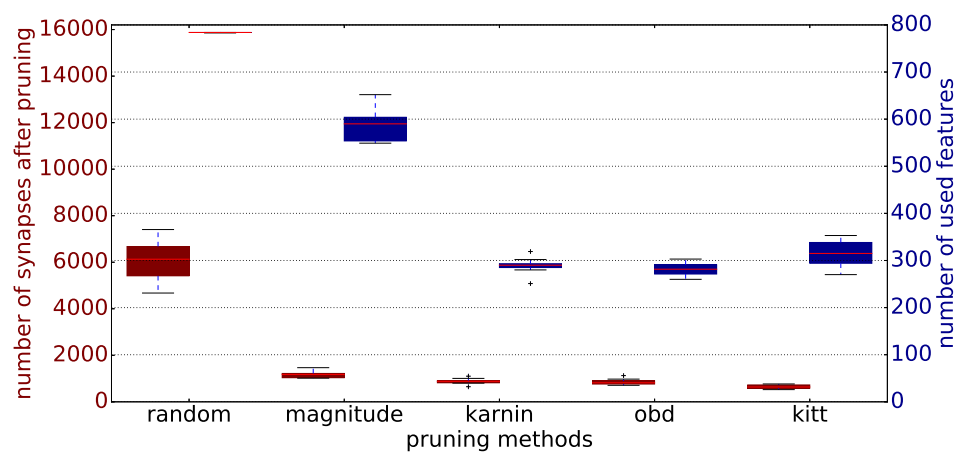


FIGURE 4.1: MNIST, req\_acc = 0.95, retraining: 5 epochs

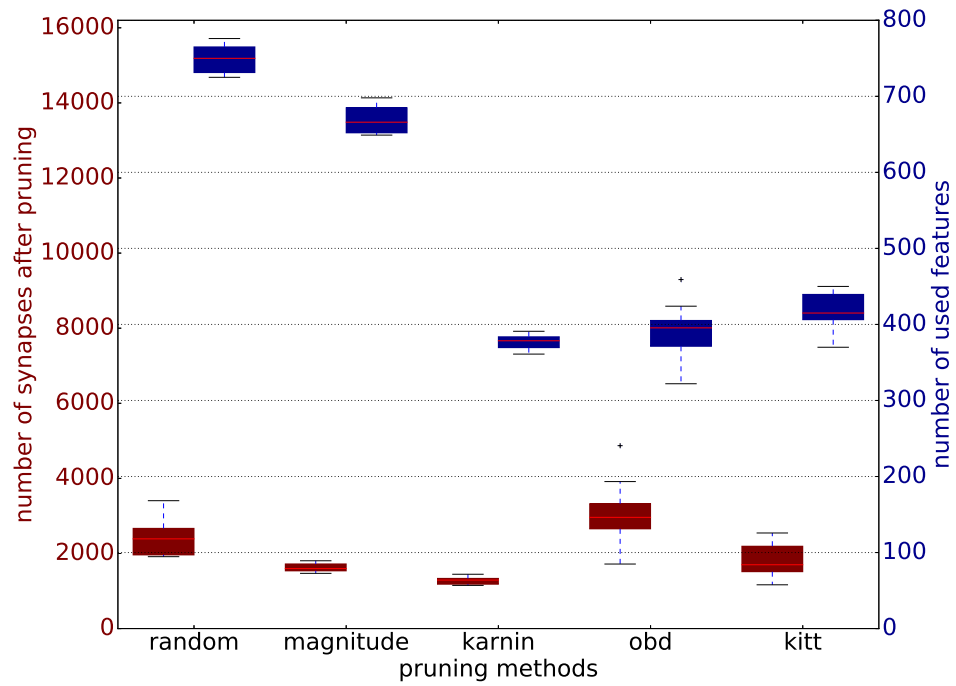


FIGURE 4.2: MNIST, req\_acc = 0.95, no retraining

### 4.3 Future Work

Outlook...

Shrinking of layers

Tailoring

Building net from zero

Sphere neuron



## Chapter 5

# Conclusion

Conclusion text...

Outlook text... shrinking layers?

# Bibliography

- [1] Frank Rosenblatt. “The perceptron: A probabilistic model for information storage and organization in the brain”. In: *Psychological Review* 65 (1958), pp. 386–408.
- [2] J. Larson and R. S. Michalski. “Inductive Inference of VL Decision Rules”. In: *ACM SIGART Bulletin*. New York, USA: ACM SIGAI, 1977, pp. 38–44.
- [3] Michael C. Mozer and Paul Smolensky. “Skeletonization: A Technique for Trimming the Fat from a Network via Relevance Assessment”. In: *Boulder*. Institute of Cognitive Science, University of Colorado: CO 80309-0430, 1989, pp. 107–115.
- [4] Ehud D. Karnin. “A Simple Procedure for Pruning Back-Propagation Trained Neural Networks”. In: *Letters. IEEE Transaction on Neural Networks*, 1990, pp. 239–242.
- [5] R. Reed. “Pruning Algorithms - A Survey”. In: *IEEE Transactions on Neural Networks (Volume:4 , Issue: 5)* (Sept. 1993), pp. 740–747. URL: <http://ieeexplore.ieee.org/xpl/articleDetails.jsp?arnumber=248452>.
- [6] Yann LeCun and Corinna Cortes. *The MNIST database of handwritten digits*. 1998. URL: <http://yann.lecun.com/exdb/mnist/>.
- [7] Wikipedia. *Plagiarism — Wikipedia, The Free Encyclopedia*. [Online; accessed 15-April-2017]. 2004. URL: [https://en.wikipedia.org/wiki/MNIST\\_database](https://en.wikipedia.org/wiki/MNIST_database).
- [8] Peter Bradley. *The XOR Problem and Solution*. 2006. URL: [http://www.mind.ilstu.edu/curriculum/artificial\\_neural\\_net/xor\\_problem\\_and\\_solution.php](http://www.mind.ilstu.edu/curriculum/artificial_neural_net/xor_problem_and_solution.php).
- [9] James Lyons. *Mel Frequency Cepstral Coefficient (MFCC) tutorial*. 2009. URL: <http://practicalcryptography.com/miscellaneous/machine-learning/guide-mel-frequency-cepstral-coefficients-mfccs/>.
- [10] Lars Buitinck et al. “API design for machine learning software: experiences from the scikit-learn project”. In: *ECML PKDD Workshop: Languages for Data Mining and Machine Learning*. 2013, pp. 108–122.
- [11] Martin Bulín. “Classification of Terrain based on Proprioception and Tactile Sensing for Multi-legged Walking Robot”. MA thesis. Campusvej 55, 5230 Odense M: University of Southern Denmark, 2016.
- [12] Michael Nielsen. *Neural Networks and Deep Learning*. 2017. URL: <http://neuralnetworksanddeeplearning.com/>.
- [13] *United States Census Bureau*. 2017. URL: <https://www.census.gov/>.
- [14] Luboš Šmídl. personal communication. supervision of the thesis. 2017.

# Appendix A1

## Supplementary Data

### Generated Speech Datasets

<i>id</i>	<i>bs</i>	<i>cs</i>	<i>ns</i>	<i>incomplete classes</i>	<i>total</i>	<i>train</i>	<i>devel</i>	<i>test</i>
ds_00	0	0	1K	F (683)	39683	31747	3968	3968
ds_01	0	1	1K	F (683)	39683	31747	3968	3968
ds_02	0	2	1K	F (683)	39683	31747	3968	3968
ds_03	0	3	1K	F (683)	39683	31747	3968	3968
ds_04	0	4	1K	F (683)	39683	31747	3968	3968
ds_05	0	5	1K	F (683)	39683	31747	3968	3968
ds_06	0	6	1K	F (683)	39683	31747	3968	3968
ds_07	0	7	1K	F (683)	39683	31747	3968	3968
ds_08	0	8	1K	F (683)	39683	31747	3968	3968
ds_09	0	9	1K	F (683)	39683	31747	3968	3968
ds_10	1	0	1K	F (589)	39589	31672	3959	3958
ds_11	1	1	1K	F (589)	39589	31672	3959	3958
ds_12	1	2	1K	F (589)	39589	31672	3959	3958
ds_13	1	3	1K	F (589)	39589	31672	3959	3958
ds_14	1	4	1K	F (589)	39589	31672	3959	3958
ds_15	1	5	1K	F (589)	39589	31672	3959	3958
ds_16	1	6	1K	F (589)	39589	31672	3959	3958
ds_17	1	7	1K	F (589)	39589	31672	3959	3958
ds_18	1	8	1K	F (589)	39589	31672	3959	3958
ds_19	1	9	1K	F (589)	39589	31672	3959	3958
ds_20	2	0	1K	F (498)	39498	31599	3950	3949
ds_21	2	1	1K	F (498)	39498	31599	3950	3949
ds_22	2	2	1K	F (498)	39498	31599	3950	3949
ds_23	2	3	1K	F (498)	39498	31599	3950	3949
ds_24	2	4	1K	F (498)	39498	31599	3950	3949
ds_25	2	5	1K	F (498)	39498	31599	3950	3949
ds_26	2	6	1K	F (498)	39498	31599	3950	3949
ds_27	2	7	1K	F (498)	39498	31599	3950	3949
ds_28	2	8	1K	F (498)	39498	31599	3950	3949
ds_29	2	9	1K	F (498)	39498	31599	3950	3949
ds_30	3	0	1K	F (410)	39410	31528	3941	3941
ds_31	3	1	1K	F (410)	39410	31528	3941	3941
ds_32	3	2	1K	F (410)	39410	31528	3941	3941
ds_33	3	3	1K	F (410)	39410	31528	3941	3941
ds_34	3	4	1K	F (410)	39410	31528	3941	3941
ds_35	3	5	1K	F (410)	39410	31528	3941	3941
ds_36	3	6	1K	F (410)	39410	31528	3941	3941
ds_37	3	7	1K	F (410)	39410	31528	3941	3941
ds_38	3	8	1K	F (410)	39410	31528	3941	3941
ds_39	3	9	1K	F (410)	39410	31528	3941	3941
ds_40	4	0	1K	F (327)	39327	31462	3933	3932
ds_41	4	1	1K	F (327)	39327	31462	3933	3932

<i>id</i>	<i>bs</i>	<i>cs</i>	<i>ns</i>	<i>incomplete classes</i>	<i>total</i>	<i>train</i>	<i>devel</i>	<i>test</i>
ds_42	4	2	1K	F (327)	39327	31462	3933	3932
ds_43	4	3	1K	F (327)	39327	31462	3933	3932
ds_44	4	4	1K	F (327)	39327	31462	3933	3932
ds_45	4	5	1K	F (327)	39327	31462	3933	3932
ds_46	4	6	1K	F (327)	39327	31462	3933	3932
ds_47	4	7	1K	F (327)	39327	31462	3933	3932
ds_48	4	8	1K	F (327)	39327	31462	3933	3932
ds_49	4	9	1K	F (327)	39327	31462	3933	3932
ds_50	5	0	1K	F (253)	39253	31403	3925	3925
ds_60	6	0	1K	D, F, N, Q, R, T	38049	30441	3805	3803
ds_70	7	0	1K	D, F, N, Q, R, T, Z	36140	28914	3614	3612
ds_80	8	0	1K	D, F, N, Q, R, T, Z	34869	27899	3487	3483
ds_90	9	0	1K	D, F, N, Q, R, T, Z, b	33680	26947	3368	3365
ds_5K	3	3	5K	D, F, N, Q, R, T, Y, Z, g	184750	147803	18475	18472
ds_10K	3	3	10K	D, F, N, Q, R, T, U, Y, Z, g, x	335812	268654	33581	33577

TABLE A1.1: Datasets generated for the *Phonemes* example (section 3.6).

## Finding Speech Dataset Params - complete results

<i>dataset id</i>	<i>job 1</i>	<i>job 2</i>	<i>job 3</i>	<i>job 4</i>	<i>job 5</i>	<i>mean</i>	<i>std</i>
ds_00	0.0112	0.0113	0.0117	0.0114	0.0114	0.0114	0.0002
ds_01	0.0116	0.0116	0.0114	0.0116	0.0115	0.0115	0.0001
ds_02	0.0114	0.0115	0.0114	0.0115	0.0116	0.0115	0.0
ds_03	0.0116	0.0114	0.0115	0.0118	0.0117	0.0116	0.0001
ds_04	0.0117	0.0117	0.0119	0.0117	0.0121	0.0118	0.0002
ds_05	0.0116	0.0118	0.0117	0.0116	0.0117	0.0117	0.0001
ds_06	0.0118	0.0119	0.0116	0.0118	0.0117	0.0118	0.0001
ds_07	0.0118	0.0117	0.012	0.0118	0.0119	0.0118	0.0001
ds_08	0.012	0.0121	0.0116	0.0118	0.012	0.0119	0.0002
ds_09	0.012	0.0119	0.0119	0.0119	0.0119	0.0119	0.0
ds_00	0.0112	0.0113	0.0117	0.0114	0.0114	0.0114	0.0002
ds_01	0.0116	0.0116	0.0114	0.0116	0.0115	0.0115	0.0001
ds_02	0.0114	0.0115	0.0114	0.0115	0.0116	0.0115	0.0
ds_03	0.0116	0.0114	0.0115	0.0118	0.0117	0.0116	0.0001
ds_04	0.0117	0.0117	0.0119	0.0117	0.0121	0.0118	0.0002
ds_05	0.0116	0.0118	0.0117	0.0116	0.0117	0.0117	0.0001
ds_06	0.0118	0.0119	0.0116	0.0118	0.0117	0.0118	0.0001
ds_07	0.0118	0.0117	0.012	0.0118	0.0119	0.0118	0.0001
ds_08	0.012	0.0121	0.0116	0.0118	0.012	0.0119	0.0002
ds_09	0.012	0.0119	0.0119	0.0119	0.0119	0.0119	0.0
ds_10	0.0114	0.0114	0.0112	0.0113	0.0114	0.0113	0.0001
ds_11	0.0114	0.0115	0.0115	0.0111	0.0117	0.0115	0.0002
ds_12	0.0113	0.0115	0.0113	0.0114	0.011	0.0113	0.0002
ds_13	0.0115	0.0115	0.0116	0.0114	0.0117	0.0115	0.0001
ds_14	0.0118	0.0115	0.0115	0.0113	0.0116	0.0115	0.0002
ds_15	0.0116	0.0119	0.0119	0.0116	0.0115	0.0117	0.0002
ds_16	0.0117	0.012	0.0118	0.0112	0.0118	0.0117	0.0003
ds_17	0.0119	0.0119	0.0118	0.0118	0.0114	0.0118	0.0002
ds_18	0.0118	0.0118	0.0116	0.0116	0.0116	0.0117	0.0001

<i>dataset id</i>	<i>job 1</i>	<i>job 2</i>	<i>job 3</i>	<i>job 4</i>	<i>job 5</i>	<i>mean</i>	<i>std</i>
ds_19	0.0118	0.0118	0.0118	0.0119	0.0117	0.0118	0.0001
ds_20	0.0112	0.0112	0.011	0.0112	0.011	0.0111	0.0001
ds_21	0.0111	0.0114	0.0113	0.0111	0.0113	0.0112	0.0001
ds_22	0.0111	0.0108	0.0109	0.0114	0.011	0.011	0.0002
ds_23	0.0109	0.0116	0.0113	0.011	0.0114	0.0112	0.0002
ds_24	0.011	0.0114	0.0116	0.0113	0.0113	0.0113	0.0002
ds_25	0.0115	0.0118	0.0113	0.0114	0.0114	0.0115	0.0002
ds_26	0.0116	0.0116	0.0117	0.0114	0.0115	0.0115	0.0001
ds_27	0.0113	0.0116	0.011	0.0117	0.0113	0.0114	0.0002
ds_28	0.0114	0.0112	0.0114	0.0111	0.0116	0.0114	0.0002
ds_29	0.0114	0.0118	0.0117	0.0118	0.0117	0.0117	0.0001
ds_30	0.0104	0.0105	0.0108	0.0105	0.0108	0.0106	0.0002
ds_31	0.0107	0.0109	0.0114	0.0108	0.0109	0.0109	0.0002
ds_32	0.0113	0.0112	0.0109	0.0112	0.011	0.0111	0.0002
ds_33	0.0111	0.0108	0.0106	0.0109	0.0109	0.0109	0.0002
ds_34	0.011	0.0113	0.0111	0.0112	0.0111	0.0112	0.0001
ds_35	0.0109	0.011	0.0112	0.0111	0.0115	0.0111	0.0002
ds_36	0.0114	0.0109	0.0112	0.0114	0.0115	0.0113	0.0002
ds_37	0.011	0.011	0.0112	0.0112	0.011	0.0111	0.0001
ds_38	0.0115	0.0113	0.0114	0.0113	0.0116	0.0114	0.0001
ds_39	0.0112	0.0111	0.0109	0.0116	0.0114	0.0113	0.0003
ds_40	0.011	0.0111	0.0107	0.0108	0.0108	0.0109	0.0001
ds_41	0.0108	0.0107	0.0111	0.0112	0.011	0.011	0.0002
ds_42	0.0111	0.0114	0.0111	0.0112	0.0112	0.0112	0.0001
ds_43	0.0111	0.0112	0.0115	0.0105	0.0112	0.0111	0.0003
ds_44	0.0108	0.0106	0.0112	0.0109	0.011	0.0109	0.0002
ds_45	0.0112	0.011	0.0107	0.0112	0.0109	0.011	0.0002
ds_46	0.0105	0.0112	0.0115	0.0112	0.0108	0.011	0.0003
ds_47	0.0112	0.0116	0.011	0.0112	0.0115	0.0113	0.0002
ds_48	0.0116	0.0115	0.0113	0.0113	0.0108	0.0113	0.0003
ds_49	0.0114	0.011	0.0115	0.0109	0.0114	0.0112	0.0003
ds_50	0.0107	0.0109	0.0107	0.0108	0.0108	0.0108	0.0001
ds_51	0.011	0.011	0.011	0.0109	0.0113	0.011	0.0001
ds_52	0.0107	0.0112	0.0109	0.011	0.0111	0.011	0.0002
ds_53	0.0108	0.0107	0.0114	0.0108	0.0109	0.0109	0.0003
ds_54	0.011	0.011	0.0113	0.011	0.0115	0.0111	0.0002
ds_55	0.0112	0.0116	0.0111	0.0112	0.0112	0.0113	0.0002
ds_56	0.0111	0.0113	0.0109	0.0108	0.011	0.011	0.0001
ds_57	0.011	0.0109	0.0105	0.011	0.0108	0.0108	0.0002
ds_58	0.0106	0.0112	0.0114	0.0108	0.0108	0.011	0.0003
ds_59	0.0112	0.011	0.0114	0.0111	0.0112	0.0112	0.0001

TABLE A1.2: Complete results of finding speech dataset parameters  $bs$  and  $cs$ . MSE' (Eq. (2.19)) after training.

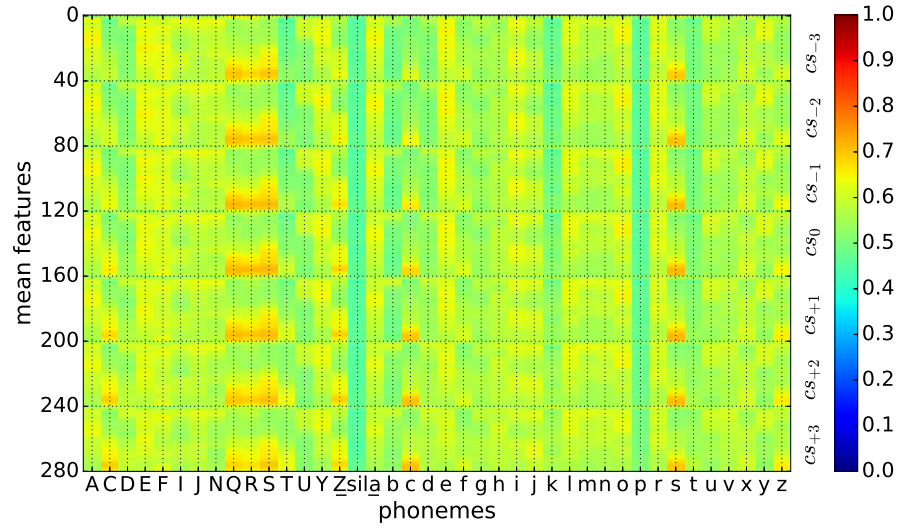
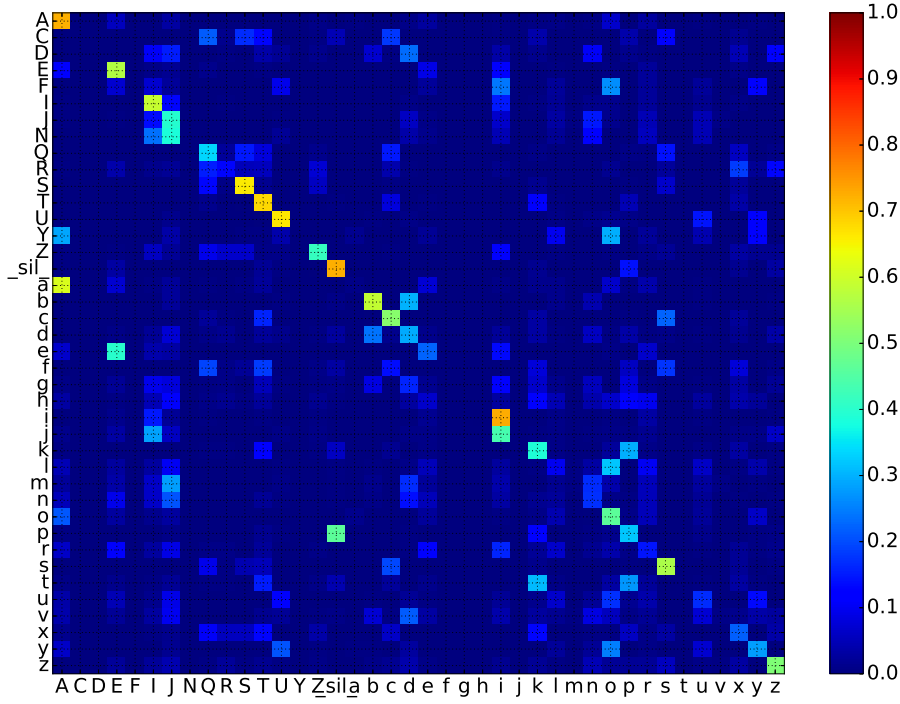
FIGURE A1.1: Average sample for each phoneme,  $cs = 3$ .

FIGURE A1.2: Trained bottleneck network (speech dataset): confusion matrix.

## Appendix A2

# Structure of the Workspace

## Appendix A3

# Implementation



## Appendix A4

# Code Documentation